

MFN 06-013
Enclosure 2

ENCLOSURE 2

MFN 06-013

NEDO-33082, Revision 1 “ESBWR Scaling Report,”

January 2006

NEDO-33082
Revision 1
Class I
eDRF 0000-0050-0037
January 2006

ESBWR Scaling Report

R.E. Gamble
A.F. Fanning
B. Vaishnavi

Approved: _____



D. Hinds, Manager
ESBWR Engineering

NON PROPRIETARY VERSION

This document is the non proprietary version of NEDC-33082P, Revision 1. Proprietary information that has been extracted is indicated by sidebars in the right margin.

**IMPORTANT NOTICE REGARDING
CONTENTS OF THIS REPORT
PLEASE READ CAREFULLY**

Neither the General Electric Company nor any of the contributors to this document:

a. Makes any warranty or representation, express or implied, with respect to the accuracy, completeness, or usefulness of the information contained in this document, or that the use of any information, apparatus, method, or process disclosed in this document may not infringe privately owned rights;

or

b. Assumes any liabilities, including but not limited to nuclear liability, with respect to the use of, or for damages resulting from the use of any information, apparatus, method, or process disclosed in this document.

This work was performed partially as part of a contract between various utilities and GE for "ESBWR Development".

REVISION 1

Revision 1 incorporates changes requested to respond to NRC Requests for Additional Information (RAIs) related to Rev. 0. All changes between Rev 0 and Rev 1 are accompanied by left side vertical change bars. Errors in Tables (A1 to A14) have been corrected. These do not affect any conclusions reached in the reports.

Table of Contents

Table of Contents	vii
List of Tables	ix
List of Figures	x
Nomenclature and Abbreviations	xi
Executive Summary	xvi
1.0 Introduction	1-1
1.1 Background	1-1
1.2 Objectives and Scope of Scaling Analysis	1-2
1.2.1 Accidents and Accident Phases Considered	1-2
2.0 Scaling Methodology	2-1
2.1 The H2TS Scaling Methodology	2-1
2.2 Scaling Laws for Test Design	2-2
2.3 Scaling for PIRT Validation and Confirmation of Test Validity	2-2
2.4 Time Scales – Closure with H2TS	2-3
3.0 System Modeling Equations	3-1
3.1 Vessel Pressurization Rate Equation for a Control Volume	3-1
3.2 Generic Junction Flow Rate Equation	3-4
3.3 Summary	3-5
4.0 Scaling for Test Design	4-1
4.1 Top down Scaling	4-1
4.2 Phase Changes at Interfaces	4-4
4.3 General Scaling Criteria	4-5
4.4 Scaling of the Piping	4-9
4.5 Compressibility of the Gas Flowing in Pipes	4-10
4.6 Time Scales	4-11
4.7 Specific Frequencies of the Process	4-14
4.8 Summary	4-15
5.0 System Descriptions	5-1
5.1 Introduction	5-1
5.2 Post-LOCA Response of the ESBWR	5-2
5.3 GIST	5-3
5.3.1 Facility Description	5-3
5.3.2 Initial Conditions and Test Control	5-3
5.4 GIRAFFE	5-4
5.4.1 Facility Description	5-4
5.4.2 GIRAFFE/SIT Tests	5-5
5.4.3 GIRAFFE/Helium Tests	5-5
5.5 PANDA	5-6
5.5.1 Facility Description	5-6
5.5.1.1 Vessels	5-7
5.5.1.2 PCCS/ICS	5-8

Table of Contents (cont'd)

5.5.1.3	Flow Paths Between Vessels	5-9
5.5.1.4	Vessel Heat Capacity and Heat Losses	5-9
5.5.2	Establishment of Test Initial Conditions	5-9
5.6	PANTHERS	5-10
5.7	UCB and MIT Condensation Heat Transfer Tests	5-10
6.0	Scaling for PIRT Validation and Test Facility Evaluation	6-1
6.1	Scaling for Important Phenomena and Facility Distortions	6-1
6.2	Global Momentum Scaling	6-7
6.3	Summary	6-7
7.0	ESBWR Results – PIRT Validation	7-1
7.1	Transient Phases	7-1
7.2	Important System Parameters	7-1
7.3	Reference Parameters	7-2
7.3.1	Transient Phase Boundaries	7-3
7.3.2	Reference Times	7-5
7.3.3	Pressure	7-5
7.3.4	Flow rates	7-6
7.4	Format of Results	7-6
7.5	Top-Down Results	7-7
7.5.1	RPV Behavior	7-7
7.5.2	Containment behavior	7-9
7.5.2.1	Drywell Pressure Rate	7-9
7.5.2.2	Wetwell Pressure Rate	7-10
7.5.2.3	Passive Containment Cooling System (PCCS)	7-11
7.5.3	Summary of Top-down Results	7-11
7.6	Bottom-up Scaling	7-11
8.0	Test Facility Scaling	8-1
8.1	Criteria for Well Scaled Facility	8-2
8.2	Reference Parameters	8-2
8.3	Short-term RPV Behavior	8-2
8.4	Long-term	8-4
8.5	PCC Scaling	8-5
8.6	Summary for Test Facility Comparison	8-5
9.0	Effect of Scale	9-1
10.0	Summary and Conclusions	10-1
11.0	References	11-1
Appendix A	Detailed Results	A-1

List of Tables

Table 5-1 The ESBWR Related Tests	5-12
Table 6-1 Summary of PI-groups	6-9
Table 7-1 Application of Scaling Equations to ESBWR Phases and Regions	7-2
Table 8-1 Numerical Scaling Evaluations	8-1

List of Figures

Figure 1-1	Key Variables and Test Coverage During ESBWR LOCA Phases	1-4
Figure 3-1	Control Volume Receiving Mass Flow Rates W_i with Corresponding Total Enthalpies h_{oi} and Heat at Rate Q	3-2
Figure 3-2	Junction Pipes	3-5
Figure 5.1	Main Components of the GIST Facility	5-13
Figure 5.2	Vessel Pressure Coastdown During the SBWR and the GIST Depressurization Transients	5-14
Figure 5-3	GIRAFFE Test Facility Schematic (GIRAFFE/SIT Test)	5-15
Figure 5-4	PANDA Test Facility Schematic	5-16
Figure 5-5	Comparison of the PANDA Elevations with the ESBWR	5-17
Figure 5-6	The PANDA PCCS and ICS Condenser Units	5-18
Figure 5-7	Passive Containment Condenser Tested at PANTHERS	5-19
Figure 5-8	Isolation Condenser Module Tested at PANTHERS	5-19
Figure 5-9	Schematic of the PANTHERS PCC Test Facility	5-20
Figure 5-10	Schematics of the PANTHERS IC Test Facility	5-21
Figure 7-1	ESBWR - RPV Late Blowdown: Time Rate of Liquid Mass Change ($M\dot{m}$)	7-13
Figure 7-2	ESBWR - RPV GDCS Transition: Time Rate of Liquid Mass Change ($M\dot{m}$)	7-14
Figure 7-3	ESBWR - RPV Full GDCS (Reflood): Time Rate of Liquid Mass Change ($M\dot{m}$)	7-15
Figure 7-4	ESBWR - RPV Late Blowdown: Time Rate of Pressure Change ($P\dot{m}$)	7-16
Figure 7-5	ESBWR - RPV GDCS Transition: Time Rate of Pressure Change ($P\dot{m}$)	7-17
Figure 7-6	ESBWR - Drywell Long Term/PCCS: Time Rate of Pressure Change ($P\dot{m}$)	7-18
Figure 7-7	ESBWR - Wetwell Long Term/PCCS: Time Rate of Pressure Change ($P\dot{m}$)	7-19
Figure 8-1	RPV Late Blowdown: Time Rate of Liquid Mass Change ($M\dot{m}$) - Summary	8-7
Figure 8-2	RPV GDCS Transition: Time Rate of Liquid Mass Change ($M\dot{m}$) - Summary	8-8
Figure 8-3	RPV Full GDCS (Reflood): Time Rate of Liquid Mass Change ($M\dot{m}$) - Summary	8-9
Figure 8-4	RPV Late Blowdown: Time Rate of Pressure Change ($P\dot{m}$) - Summary	8-10
Figure 8-5	RPV GDCS Transition: Time Rate of Pressure Change ($P\dot{m}$) - Summary	8-11
Figure 8-6	Drywell Long Term/PCCS: Time Rate of Pressure Change ($P\dot{m}$) - Summary	8-12
Figure 8-7	Wetwell Long Term/PCCS: Time Rate of Pressure Change ($P\dot{m}$) - Summary	8-13
Figure 9-1	Nondimensional RPV Pressure Comparison for SBWR, GIRAFFE/SIT and GIST	9-2
Figure 9-2	Nondimensional RPV Liquid Mass Comparison for SBWR, GIRAFFE/SIT and GIST	9-3
Figure 9-3	Comparison of WW Pressure Increases with Noncondensable Partial Pressures for Giraffe/He, PANDA-M and PANDA-P tests	9-4
Figure 9-4	Comparison of PCC and IC Behavior for Pure Steam at Different Scales	9-5
Figure 9-5	Comparison of PCC Behavior for Steam-Noncondensable Mixtures at Different Scales	9-6

Nomenclature and Abbreviations

Symbols	Description	Units
A	Surface area	m^2
a	Cross-sectional area	m^2
c_p	Specific heat at constant pressure	J/kg K
c_v	Specific heat at constant volume	J/kg K
d	Characteristic length	m
D	Diameter	m
E	Internal energy	J
e	Specific internal energy	J/kg
f	Darcy friction factor	*
F_n	Loss coefficient for pipe segment (Eq. 3.2-2b)	*
F/a^2	Sum of loss coefficients divided by area ² (Eq. 3.2-4b)	$1/m^4$
H	Height or submergence	m
h	heat transfer coefficient	W/m^2K
h	Specific enthalpy	J/kg
h_{fg}	Latent heat of vaporization	J/kg
G	Mass flux	kg/m^2s
g	Acceleration of gravity	$9.81 m/s^2$
j, J	Volumetric flow rate	m^3/s
k	Ratio of specific heats, c_p/c_v	*
k	Thermal conductivity	W/mK
k_n	Local loss coefficient of segment n	*
λ_n	Length of segment	m
L/a	Sum of lengths divided by areas (Eq. 3.2-4c)	$1/m$
L	Length	m
M	Mass	kg
\dot{m}	Mass flow rate	kg/s
P	Pressure	Pa
ρ	perimeter	m
\dot{Q}	Heat rate	W
R	Gas Constant	J/kgK
R	System Scale (prototype to model)	*
T	Temperature	K

* = dimensionless

Nomenclature and Abbreviations (cont'd)

t	Time	s
u	Velocity	m/s
V	Volume	m ³
v	Specific volume	m ³ /kg
W	Mass flow rate	kg/s
y	Mass fraction	*
z	Axial coordinate along flow path	m
Bi = h d/k _s	Biot number	*
Fo	Fourier number	*
Nu = h d/k	Nusselt number	*

Greek Letters

Symbols	Description	Units
Δ	Change in reference parameter	
α	Void fraction	*
μ	Viscosity	kg/m s
Π	Nondimensional group	*
ρ	Density	kg/m ³
τ	Time constant	s
ω	Characteristic frequency	s ⁻¹
∂	Partial differential operator	
Γ	Net vaporization rate	kg/m ³ -s
ψ	Vapor mass function	*
Σ	Summation	

Subscripts

Symbols	Description
Decay	Decay heat
e	Energy equation PI group
g	Gas
g	gravity
h	Submergence or hydrostatic head term
hp	Enthalpy-pressure
IC	Isolation condenser
i	Mass flow path (for summations)
in	Inertia
j	constituent (for summations)
k	Sensible energy flow path (for summations)

* = dimensionless

Nomenclature and Abbreviations (cont'd)

L, λ	Liquid
LG	Change from liquid to gas
loss	Friction and form loss
M	Mass
M	Mass equation PI group
MV	Main Vent
mech	Mechanical compression due to mass addition term
mod	Model or test facility
m	generic junction pipe
n	Pipe segment
nv	Vertical portion of pipe segment
o	Initial value
P	Pressure rate equation PI group
PCC	Passive Containment Cooling Condenser
PCCS	Passive Containment Cooling System
\dot{P}	Flashing term
\dot{P}_1	Flashing term
\dot{P}_2	Flashing term
p	Pipe
pch	Phase change
pd	Pressure difference
prot	Prototype or ESBWR
R	Reactor pressure vessel, scale factor between prototype and model
RPV	Reactor Pressure Vessel
r	Reference parameter
sub	Subcooling or submergence
v	Refers to vertical distance
VB	Vacuum breaker
W	Flow
Wh	Energy flow due to enthalpy
\dot{Q}	Energy rate
\dot{V}	Volume change

Additional subscripts are defined in the text.

Nomenclature and Abbreviations (cont'd)**Superscripts****Symbols Description**

'	Denotes derivative with respect to pressure
.	Denotes derivative with respect to time
+	Nondimensional variable

Abbreviations**Symbols Description**

ADS	Automatic Depressurization System
BAF	Bottom of Active Fuel
CHF	Critical Heat Flux
DBA	Design Basis Accident
DPV	Depressurization Valve
DW	Drywell
ESBWR	Economic Simplified Boiling Water Reactor
GDCS	Gravity-Driven Cooling System
GDLB	GDCS line break
GE	General Electric Company
GIST	GDCS Integrated Systems Test
H2TS	Hierarchical Two-Tier Scaling
h.t.c.	Heat transfer coefficient
IC	Isolation Condenser
ICS	Isolation Condenser System
LOCA	Loss-of-Coolant Accident
MIT	Massachusetts Institute of Technology
MSL	Main Steam Line
MSLB	Main Steam Line Break
NB	No-Break
NRC	Nuclear Regulatory Commission
PCC	Passive Containment Condenser
PCCS	Passive Containment Cooling System
PIRT	Phenomena Identification and Ranking Table
PSI	Paul Scherrer Institute
RPV	Reactor Pressure Vessel
SBWR	Simplified Boiling Water Reactor
SC	Pressure Suppression Chamber
SIT	Systems Interaction Tests
SP	Suppression Pool
SRV	Safety/Relief Valve

Nomenclature and Abbreviations (cont'd)

TAF	Top of Active Fuel
TAPD	SBWR Test and Analysis Program Description
UCB	University of California at Berkeley
WW	Wetwell
Π	Refers to nondimensional group

EXECUTIVE SUMMARY

The **objective** of this scaling report is to show that the test facilities properly “scale” the important phenomena and processes identified in the ESBWR PIRT and/or provide assurance that the experimental observations from the test programs are sufficiently representative of ESBWR behavior for use in qualifying TRACG for ESBWR licensing calculations. This objective is met through a series of steps described below.

Section 2 provides an overview of the methodology used. The scaling methodology follows the hierarchical two-tiered scaling methodology composed of top-down scaling, which identifies processes important to the system behavior and a bottom-up, or phenomena level, scaling that looks at the characteristics of the processes identified as important from the top-down scaling

Section 3 describes the equations that govern the behavior of parameters important to the behavior and safety of the ESBWR, namely: RPV liquid mass, pressure and void fraction; containment pressure; and suppression pool energy. These equations are normalized in subsequent sections to provide scaling laws and evaluate the ESBWR and test facilities.

In **Section 4** the system governing equations are normalized using general reference parameters in order to arrive at a set of **general scaling criteria** that can be used for test facility design. These are the criteria that were used for the design of the test facilities included in this report. **Brief descriptions of the test facilities** are provided in **Section 5** as well as references to where the details of the test facilities can be found. In general the design of the experimental facilities and the conduct of the various tests were guided by consideration of the proper modeling and simulation of the key phenomena governing the performance of the passive safety systems. The implications of the scaling adjustments for the ESBWR are minimized by the fact that all of the tests were performed at prototypical temperature and pressure and with prototypical or near-prototypical elevations and elevation differences. These are the key variables and parameters governing the performance of the passive safety systems.

It should be noted that the general scaling criteria are very useful for facility design but do not provide a measure of what phenomena are important to the system behavior, nor are they useful in identifying distortions in the test facilities once they are completed. Instead this is accomplished with a more detailed nondimensionalization of the governing equations as described in **Section 6**. The nondimensionalization developed in Section 6 provides detailed scaling equations that can be used to identify which phenomena are important to the system behavior and therefore should be well scaled in the test facilities. Additionally these equations can be used to assess if this goal had been achieved in the tests.

In **Section 7** the detailed scaling equations from Section 6 are applied to the ESBWR to identify the processes important to the system behavior. The parameters important to safety are identified as: the RPV liquid mass that ensures that the core remains covered; the RPV pressure which is important in determining the timing of the GDACS injection; and the containment pressure which is important to assure that the containment is not breached during an accident. The LOCA transient is broken down into four temporal phases – late blowdown, GDACS transition, reflood, and long-term decay heat removal – within which the dominant phenomena remain unchanged and the phenomena magnitudes are relatively constant.

The **results for the ESBWR** indicate that a small number of processes are important to the behavior of the system parameters of interest (liquid mass and pressure). For the RPV liquid mass the important processes are flashing due to depressurization, boiling due to energy input from stored energy and decay heat, and GDCS flow (Figures 7-1 through 7-3). Although other parameters influence the behavior of the liquid mass during the short GDCS transition phase, the mass change during this phase is very small and therefore not very significant to the overall mass loss in the vessel. For the RPV pressure the dominant phenomena is energy flow through the ADS system (Figures 7-4 and 7-5).

The wetwell pressure controls the containment pressure and the drywell is found to be unimportant to the containment response during the transient period considered (late blowdown onward). The drywell is found to act in a manner similar to a large pipe that transfers steam from the RPV to the main vents and PCCs (Figure 7-6). The time constant for the DW pressure is very short compared to the wetwell and the pressure in the DW therefore rapidly adjusts to the boundary condition presented by the WW pressure. The primary contribution of the DW is that its volume determines the quantity of noncondensable gas that must be accommodated by the WW in the long term. The important process for the containment pressure is the movement of noncondensable gas from the DW to the WW (Figure 7-7).

In **Section 8**, the same scaling method is applied to the test facilities to evaluate if the phenomena identified as important to the ESBWR are scaled properly in the test facilities. Figures 8-1 through 8-7 show that all of the important phenomena magnitudes are well scaled in the test facilities.

Proper bottom-up scaling is a common problem with reduced scale facilities, where aspect ratio, surface to volume ratio and other geometric considerations make it difficult to simulate local effects. A review of the processes important to the system behavior concludes that they are either well scaled from the bottom-up perspective (ADS flow, PCC heat removal, SP mixing) or can be addressed through parametric studies and a bounding approach with TRACG (stratification in gas space, SP mixing). Much of the bottom-up results are borrowed from the SBWR scaling report rather than repeating them in this report.

Although it does not constitute scaling analyses, **absence of significant distortions is confirmed** by comparing key parameters from tests done at a wide variety of scales in **Section 9**. The comparisons shown in Figures 9-1 through 9-5 show a similar behavior at all scales indicating that the important processes were well represented in the tests and that no significant scale distortions occurred.

Overall the test facilities are demonstrated to adequately simulate the phenomena important to the ESBWR. Although there are distortions in the facilities, they are found to be in areas that do not affect significant parameters for the system behavior. As such, the test data obtained from these facilities are suitable for qualification of TRACG.

1.0 INTRODUCTION

1.1 Background

In the 1980's, GE began a project to design and certify a new Boiling Water Reactor (BWR) design which incorporates advanced, passive safety features. The Simplified BWR (SBWR) experienced design evolution from its beginning until the mid 1990's.

The final design was a natural circulation reactor rated at 670 MWe with a typical BWR pressure suppression containment system. The major safety systems are:

- Gravity-Driven Cooling System (GDCCS), which during a postulated loss-of-coolant accident (LOCA), supplies makeup water to the reactor core from a pool located above the core.
- Isolation Condenser System (ICS), which during an isolation transient, uses natural circulation to remove core decay heat from the reactor pressure vessel (RPV) by condensing steam from the RPV and returning condensate to the RPV.
- Passive Containment Cooling System (PCCS), which during a postulated LOCA, removes heat from the containment by condensing steam from the drywell and returns the condensate to the GDCCS pool.

A comprehensive experimental program was carried out to demonstrate the thermal-hydraulic performance of these passive systems and their components. The philosophy of testing was to focus on those features and components that are SBWR-unique or performance-critical, and to test over a range that spans and bounds the SBWR parameters of importance. In addition to demonstrating the performance of these systems, these tests were conducted to provide test data to be used to qualify the TRACG computer code for SBWR application. TRACG is the GE version of TRAC-BWR.

Major SBWR test programs were conducted at the GIST, GIRAFFE, PANTHERS, and PANDA test facilities. GIST, GIRAFFE, and PANDA were integral systems tests focusing on different aspects of the SBWR response to LOCAs. Figure 1-1 shows the relationship of these tests to the LOCA phases. These facilities also simulated the SBWR at different system scales (1:500 for GIST, 1:400 for GIRAFFE and 1:25 for PANDA). PANTHERS tests were full-scale component tests of prototypical ICS and PCCS condensers.

In the mid 1990's, GE redirected the focus of SBWR programs from plants of the 670 MWe size to plants of 1000 MWe or larger. However, GE completed key ongoing test and analysis activities to make this data available for other applications of the SBWR technology.

The larger plant design evolved into the 4500 MWt (1565 MWe) ESBWR design. The scaling data presented in this report are based on the previous ESBWR design value of 4000 MWt (1390 MWe). The ESBWR is in general a first principles scale-up of the SBWR¹. However, there are a few configuration changes to enhance the safety performance of the design as described in [1-1]. The testing done for the SBWR is still representative of the ESBWR, but at smaller scale

¹ RAI 16

(1:1000 for GIST, 1:800 for GIRAFFE and 1:50 for PANDA). To expand the experimental database, additional tests were run in the PANDA facility at a scale of 1:50, representative of the ESBWR.

The *ESBWR Test and Analysis Program Description* (TAPD) [1-2] describes a comprehensive integrated plan that addresses the testing elements needed for analysis of ESBWR performance. The TAPD provides the technical basis for determining the performance of the plant during transients and accidents. It provides the rationale for the diverse experimental and analytical efforts in support of ESBWR certification based on the Phenomena Identification and Ranking Tables (PIRT). These tables listed the phenomena and interactions between systems important to ESBWR transient and accident analysis.

This report goes on to provide an evaluation of the test facilities with respect to the scaling of the important phenomena and processes identified in the ESBWR PIRT. The study demonstrates that the experimental observations from the test programs were representative of ESBWR behavior and that the data are useful for TRACG qualification.

1.2 Objectives and Scope of Scaling Analysis

The scope of the scaling study reported here was to:

- Describe the scaling philosophy and strategy used in designing the various tests.
- Provide the applicable scaling laws.
- Identify important phenomena to ESBWR behavior and provide information for PIRT validation.
- Show that the test facilities properly “scale” the important phenomena and processes identified in the ESBWR PIRT and/or provide assurance that the experimental observations from the test programs are representative of ESBWR behavior.
- Identify scaling distortions and discuss their importance; in particular, identify the ways by which scaling distortions should be considered when the experimental data are used for code qualification.
- Provide the basis for showing that the experimental data cover the correct phenomena and ranges for qualifying TRACG for application to ESBWR accident analysis.

1.2.1 Accidents and Accident Phases Considered

The range of accidents considered includes the main steam line break (MSLB), as well as other breaks of the primary system, such as the GDCS line break and the bottom drain line break.

The scenario for these accidents can be roughly subdivided into four phases:

- The *blowdown phase* extending from the initiation of rapid depressurization by blowdown up to the time of GDCS initiation. The blowdown phase can be further

subdivided into an *early* phase extending until the time the pressure reaches a level of about 0.8 MPa, and a *late* blowdown phase thereafter.

- A *GDCS Transition phase* covering the short period from when the RPV pressure has decreased enough that the GDCS flow to the RPV begins, to the time when the GDCS flow reaches its maximum value.
- An intermediate *GDCS phase* during which the GDCS is delivering its stored water inventory to the primary system.
- A *long-term cooling phase* beginning when the RPV inventory starts becoming replenished by the condensate flowing down from the PCCS (i.e., when the GDCS hydrostatic head necessary to drive flow into the core is made up by the PCCS condensate). At about the same time, the PCCS condensers become the dominant decay heat removal mechanism, replacing the heat sink provided by the water inventory initially stored in the GDCS pools.

The scaling analysis performed in this report is primarily directed at scaling the reactor and containment components and phenomena which are significant during the time period starting with the late blowdown phase and extending into the long-term cooling phase. As stated in Section 1.1, phenomena associated with the early stage of depressurization of a BWR vessel are well understood and are not considered to be part of the ESBWR testing program. Thus, this report deals with *post-LOCA performance* focusing on the phases of the transient following the early blowdown phase.

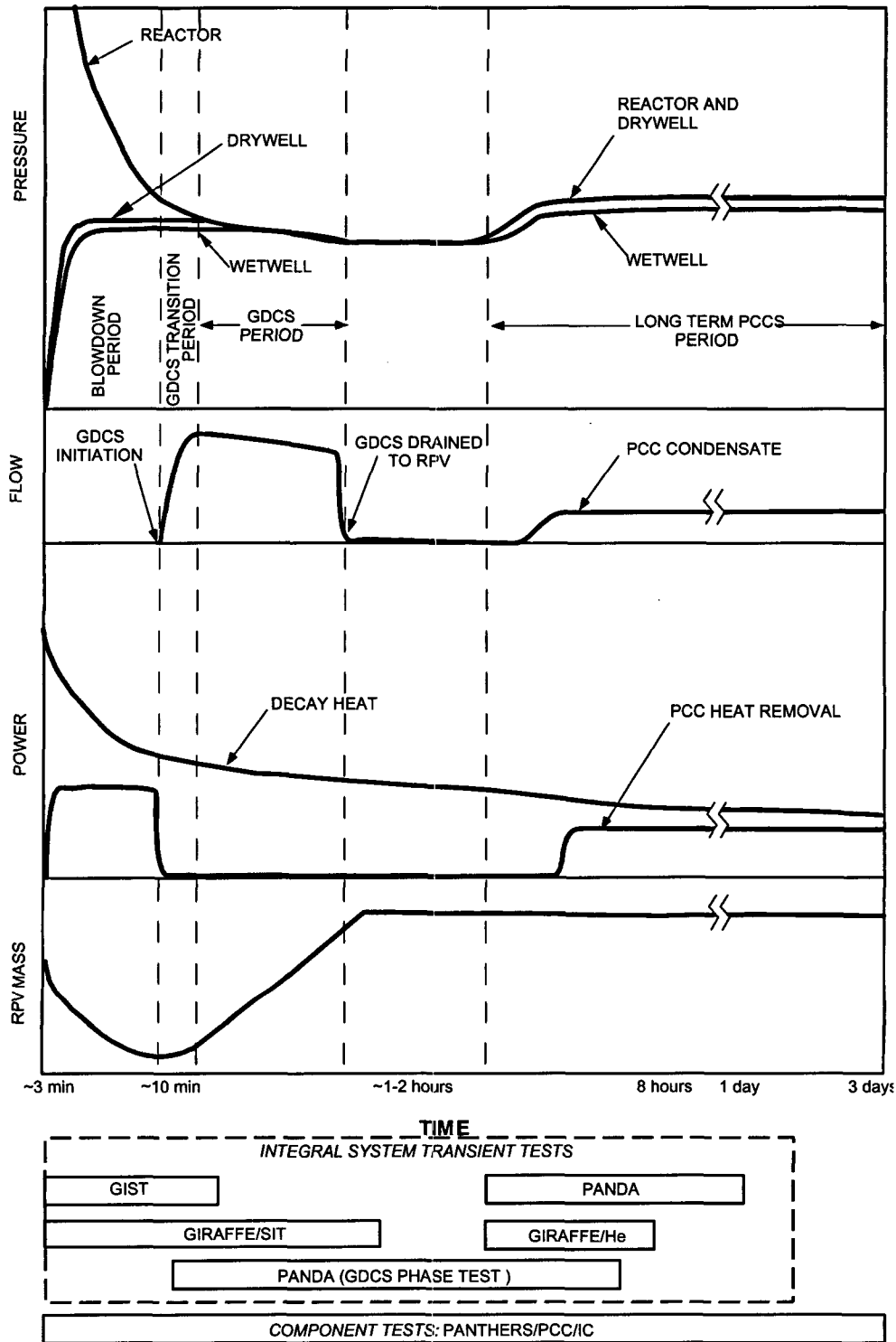


Figure 1-1 Key Variables and Test Coverage During ESBWR LOCA Phases

2.0 SCALING METHODOLOGY

2.1 The H2TS Scaling Methodology

The scaling methodology developed by an NRC Technical Program Group [2-1] was applied in this study for the purpose of evaluating the experiments and computer models in terms of how well they represent actual cooling systems and phenomena of the ESBWR.

Objectives of the NRC scaling methodology are summarized as follows:

- To provide a scaling methodology that is systematic and practical, auditable, and traceable.
- To provide the scaling rationale and similarity criteria.
- To provide a procedure for conducting comprehensive reviews of facility design, of test conditions and results.
- To ensure the prototypicality of the experimental data.
- To quantify biases due to scaling distortions or due to nonprototypical conditions.

The scaling methodology embraces the behavior of integrated subsystems and components (top-down approach), and specific processes which may occur within the subsystems (bottom-up approach).

A subsystem in the ESBWR is defined as a volume, such as the reactor vessel, drywell, wetwell air space, wetwell pool, the PCC condenser, and the isolation condenser. Global properties of a given subsystem include the pressure or the hydraulic head which drives mass flow rate, the bulk temperature differences which drive heat transfer, and the total mass and energy inflows, outflows, and storage rates. Furthermore, flow paths connecting the various volumes are included in the subsystem category because associated flow rates depend on global properties of connected volumes and resistance and inertia properties of the flow paths. Similarity laws for the ESBWR subsystems were obtained from top-down considerations.

The state within a volume may depend on phenomena that cause spatial nonuniformity in properties, such as bubble and droplet formation, density stratification of steam and noncondensibles in the drywell, or thermal plumes and stratification in both the pools and drywell. If stratification in two well-mixed superimposed layers occurs within a volume, two distinct volumes with uniform global properties will exist for the top and bottom layer subsystems formed. If complete mixing and spatial uniformity occurs within a volume, one subsystem and one global state is appropriate. If the degree of component or phase stratification varies throughout a volume, and the properties of the mass being discharged from a given location is important, it is desirable to satisfy bottom-up similarity laws which govern the stratification. Heat transfer and condensation processes in the PCCS are determined by fine-structure, local heat and mass transfer phenomena, which involve bottom-up considerations.

The magnitude of the nondimensional Π groups resulting from top-down and bottom-up scaling considerations depends on the particular LOCA phase; namely, Blowdown, GDCS Transition, Reflood and PCCS. The scaling procedure yields a unique set of Π groups for each phase, because properties at the beginning of each phase (initial states) and the dominant time responses are different.

The H2TS procedure involves writing the equations that govern the property behavior of each subsystem in the ESBWR. One set of equations gives the rates of pressurization in each volume, expressed in terms of mass and energy flow rates, and current state properties. A second set of equations provides the energy rate of change in each volume. A set of momentum equations provides the flow rate in each connecting path, ranging from transient flow when driving pressures or hydraulic heads are changing, to steady state. The details of this are shown in Section 3.

Scaling is performed by nondimensionalizing the equations governing a particular process or phase of an accident. This is accomplished classically by dividing the (dimensional) values by reference values or scales to make them nondimensional. The nondimensional variables and the various scales are then separated in two groups: (1) groups of reference scales, and (2) the so-called Π groups or Π numbers, which appear and multiply the nondimensional terms. Two parallel approaches are used for nondimensionalizing the governing equations. The first is appropriate for test facility design and results in a set of general scaling criteria that can be used in the design of test facilities. The second approach is appropriate for confirming the adequacy of test data for use in representing a specific plant system. This second approach results in an identification of important phenomena and a measure of distortions between the tests and prototype. These two approaches are summarized below and described in detail in Sections 4 and 6, respectively.

2.2 Scaling Laws for Test Design

If a test facility is perfectly scaled, then the values of all Π numbers for the prototype and the model should be perfectly matched². By considering a priori perfect matching of all the Π numbers for all system components, one can obtain guidance regarding *general scaling criteria*. In deriving such general scaling criteria, one does not have to worry in particular about the magnitude of the *nondimensionalized* terms, since everything should in principle be perfectly matched. This is the analysis described in Section 4. It leads to the *general* criteria that govern scaling of the models.

The test facilities for the ESBWR test program have been designed following this basic philosophy. The resulting test facilities, as well as the ESBWR are summarized in Section 5.

2.3 Scaling for PIRT Validation and Confirmation of Test Validity

In practical cases, the model cannot be perfectly scaled. One then needs to evaluate the importance of scaling distortions. These appear as differences in the values of the pairs of Π groups calculated for the various components of the system (prototype and model). Since, for a given system and a specific Π number, several pairs of Π values may need to be calculated, the range of magnitudes that pairs of a *particular* Π group may take may be broad. For example, when Π groups containing the various flow rates entering into a control volume are considered, the magnitude of a *component* Π group will depend on the magnitude of the corresponding flow rate. To properly evaluate the magnitude of scaling distortions, in defining the Π numbers, one should use reference scales making the magnitude of all the *nondimensional* terms of order one.

² RAI 253

The Π numbers multiplying the various nondimensional terms specify their relative importance in the governing equation. In addition comparing corresponding Π numbers between the test and prototype result in a measure of the distortion for the related phenomenon. The scaling groups developed in Section 6 for this purpose are related to, but different from, the relationships developed for the general scaling criteria in Section 4. The general scaling criteria are general relations used to design a test facility while the equations developed in Section 6 are used to identify the important phenomena in the ESBWR and quantify distortions present in test facilities. The equations in Section 4 result in the minimum number of scaling groups that must be maintained in order to adequately scale the prototype with a test facility. There is no attempt to minimize the groups developed in Section 6 although many of them are combinations of other scaling groups. The application is much clearer if each scaling group is spelled out as a new group. The equations in Section 6 satisfy two purposes: first, identifying the important phenomena to the ESBWR behavior provides information for validating the PIRT rankings; second, the method can be applied to the test facilities after they are designed to show that the phenomena important to the ESBWR behavior have been represented adequately in the test facility. The application of these equations to the ESBWR for important phenomena identification is found in Section 7. The confirmation of test facility scaling is performed in Section 8.

2.4 Time Scales – Closure with H2TS

One possible response time during a given LOCA phase consists of a volume filling or emptying time, based on initial or other reference flow rates. Another response time is associated with the transient acceleration of an open flow loop between the reactor and wetwell, the pressure source and sink. One other response time involves the vessel decompression, and is significantly different from the water mass emptying time of that vessel.³

Another process for comparing relative time responses in an integrated system is provided in the H2TS, which involves both the time constant of subsystems and a corresponding transport frequency. That is, if a flow transient response occurs in a pipe between two volumes, the system response time would correspond to either the filling or emptying time of the controlling volume (e.g., the GDCS pool). The transport frequency would correspond to the number of purges per unit time of the GDCS pool drain line. The product of frequency and response time gives the number of purges during the filling or emptying process. When a high number of purges occurs, it is not necessary to preserve the acceleration time response of the flow path, but only the quasi-steady flow properties. When a small number of purges occurs, the flow path inertia would influence the system behavior, and it would be desirable to preserve the Π groups involving inertia.

The same result is obtained by comparing the volume fill times to the transit times of the connected piping. When the fill time is much longer than the transit time, then the flow path inertia is not important. This is the approach taken in this report, as described in Section 2.4.

³RAI 254

3.0 SYSTEM MODELING EQUATIONS

3.1 Vessel Pressurization Rate Equation for a Control Volume

Consider the control volume V of Figure 3-1⁴ containing a mass M with internal energy E at a pressure P and a temperature T ⁵. The volume contains a number of constituents (noncondensable gases, steam, etc.), each denoted by the subscript j . Any changes in the kinetic and potential energy of the mass M are much smaller than changes in its intrinsic internal energy and therefore are neglected. The system is well mixed (i.e., the distributions of constituents and of the temperature are uniform), and at thermodynamic equilibrium. The conservation equations for mass and energy are used to derive an equation for the rate of pressure change in this control volume. The conservation equations and the final result are given in this section; the details of the derivation can be found in Appendix B of reference [3-1]⁶.

The *total-mass* continuity equation for this volume is:

$$\frac{dM}{dt} - \sum_i W_i = 0 \quad (3.1-1)$$

where W_i are the total (steam, noncondensables, etc.) mass flow rates entering the volume. The mass conservation equation for *constituent j* is

$$\frac{dM_j}{dt} - \sum_i W_{i,j} = 0 \quad (3.1-2)$$

Here a constituent is either steam-water or a noncondensable gas.

The energy conservation equation is:

$$\frac{dE}{dt} = -P \frac{dV}{dt} + \mathcal{Q} + \sum_i W_i h_{o,i} \quad (3.1-3)$$

where \mathcal{Q} is the heat added to the system (e.g., by conduction through the wall), and $h_{o,i}$ is the total specific enthalpy of stream i . The total enthalpy (subscript o) includes the kinetic and potential energy. The specific internal energy of the system,

$$e = \frac{E}{M} \quad (3.1-4)$$

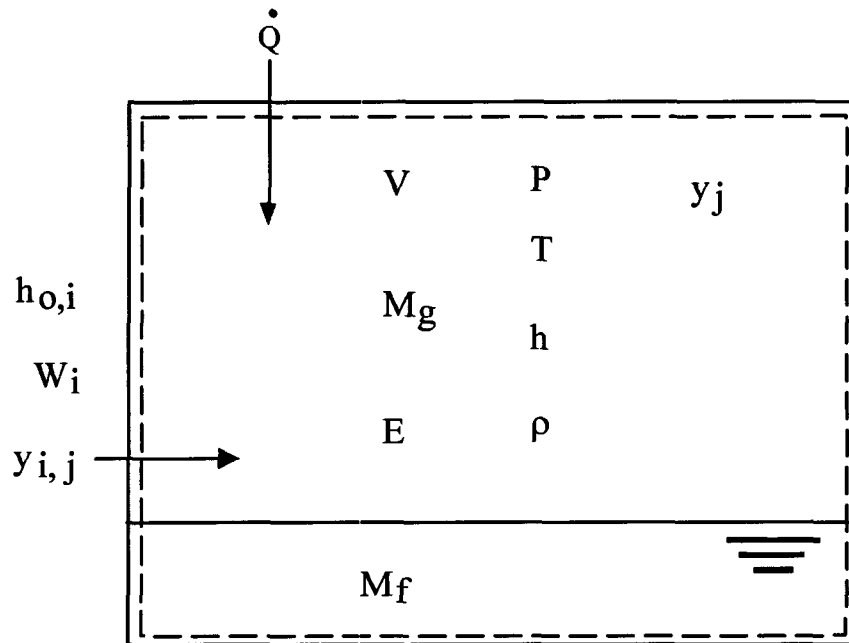
is a function of two thermodynamic variables, namely, the pressure and the specific volume $v = V/M$; and of the mass fractions y_j of the various constituents:

$$e = e(P, v, y_j) \quad (3.1-5)$$

⁴ RAI 257

⁵ RAI 255

⁶ RAI 256



$$e = \frac{E}{M} = e(P, v, y_j)$$

A containment volume receiving mass flow rates W_i with corresponding total enthalpies $h_{o,i}$ and heat at rate Q

Figure 3-1 Control Volume Receiving Mass Flow Rates W_i with Corresponding Total Enthalpies $h_{o,i}$ and Heat at Rate Q

The conservation equations and state equation listed above can be combined to derive an equation for the rate of change of the internal specific energy of the volume and an equation for the rate of pressurization, dP/dt , of a control volume. These equations were derived in Ref [3-1] and can be written in compact form as follows:

$$M \frac{de}{dt} = -P \frac{dV}{dt} + \sum_k \dot{Q}_k + \sum_i W_i (h_{o,i} - h) + \frac{P}{\rho} \sum_i W_i \quad (3.1-6)$$

$$V f_2 \frac{dP}{dt} = \sum_i [W_i (h_{o,i} - h)] + \sum_i W_i P^* v + \sum_k \dot{Q}_k - P^* \frac{dV}{dt} - V \sum_j \left[f_{1,j} \frac{dy_j}{dt} \right] \quad (3.1-7)^7$$

where the following short-hand notations were made:

$$P^* \equiv P + \left. \frac{\partial e}{\partial v} \right|_{P, y_j} \quad (3.1-8)$$

$$f_{1,j} \equiv \left. \frac{1}{v} \frac{\partial e}{\partial y_j} \right|_{P, v, y} \quad (\text{units of energy per unit volume})$$

$$f_2 \equiv \left. \frac{1}{v} \frac{\partial e}{\partial P} \right|_{v, y_j} \quad (\text{nondimensional})$$

where y_j constant means all y_j are held constant and y constant means all y_j except the one in the derivative are held constant.

For containment vapor volumes, the quantities P^* , $f_{1,j}$ and f_2 denote thermodynamic properties of the mixture, which are functions of P , v , and y_j . When prototypical fluids under prototypical thermodynamic conditions are used, these thermodynamic properties are identical for prototype and model.

We note that Equation 3.1-7 yields the rate of change of the pressure in terms of heat addition, mass and enthalpy fluxes into the volume, and changes of volume *composition*. The rate of change of volume dV/dt (e.g., due to phase change at the boundary) is also considered.

The system compliance in Equation 3.1-7 is a function of the vapor mass fraction in vessels containing liquid such as the RPV. The equation for the vapor fraction is obtained by combining the vapor phase continuity equation and net vapor generation equation⁸:

$$\rho_g \frac{d\alpha}{dt} = \frac{1}{V} \sum W_g + \frac{\sum (h_\lambda - h_f) W_\lambda}{h_{fg} V} + \frac{\mathcal{Q}}{h_{fg} V} + \frac{\psi}{h_{fg}} \frac{dP}{dt} \quad (3.1-9)$$

where

$$\psi = 1 - (1 - \alpha) \rho_f h'_f - \alpha \rho_g h'_g - \alpha h_{fg} \rho'_g \quad (3.1-10)$$

This can also be written in terms of the liquid mass equation⁹; as developed in Appendix A of [3-2] as

$$\frac{dM_l}{dt} = - \sum_k \frac{\mathcal{Q}_k}{h_{fg}} + \sum_i W_{l,i} + \sum_i \frac{\Delta h_{sub} W_{l,i}}{h_{fg}} - \frac{1}{h_{fg}} \left[V_{RPV} (1 - \rho_g h'_g) + M_l \left(\frac{\rho_g}{\rho_l} h'_g - h'_f \right) \right] \frac{dP_R}{dt} \quad (3.1-11)$$

⁸ RAI 259. The vapor generation equation is derived in Section 2.4.3 of "Two-Phase Flow in Complex Systems", by Salomon Levy, and reproduced in Appendix B of "SBWR Scaling Report", NEDC-32288P.

⁹ RAI 262

3.2 Generic Junction Flow Rate Equation

The general equation governing the pressurization rate in control volumes was developed in Section 3.1. In this section, the equation governing the flows of mass in junctions between control volumes is developed.

Mass transfers between control volumes (i.e., at flow junctions) are driven by pressure differences; these could be due to differential buildup of pressure in the two volumes attached to a junction or may be hydrostatically driven. In this section the generic equation governing junction flow rates is presented.

The general cases (Figure 3-2) of pipes connecting two volumes at pressure P_1 and P_2 are considered. The pipe in the receiving vessel may be immersed in a pool of liquid at a submergence H ; this configuration is referred to as a "vent". The case of an open vent is considered here. When the vent is closed, the column of liquid in the vent line balances the hydrostatic pressure difference between the two volumes. The case of single-phase incompressible flow is considered here, since this is the case for the majority of the junction flows in the ESBWR containment system. The case of two-phase flows can be obtained by specifying appropriate two-phase friction multipliers.

The detailed derivation of the junction flow rate equation of length λ_n starts by considering the momentum equation for time-dependent flow in a *segment* of the piping. By adding the momentum equations in different segments constituting a *flow path*, the following equation is obtained:

$$\sum_n \frac{\lambda_n}{a_n} \frac{dW}{dt} = \Delta P_{12} + \rho g \sum_n \lambda_{nv} - \rho_L g H - \sum_n \frac{F_n}{a_n^2} \frac{W^2}{2\rho} \quad (3.2-1)$$

where,

$$\Delta P_{12} = P_1 - P_2 \quad (3.2-2a)$$

and

$$F_n = \frac{f_n \lambda_n}{D_n} + k_n \quad (3.2-2b)$$

The various symbols are defined in Figure 3-2, and k_n and f_n are the local loss coefficient and friction factor, respectively, in segment n . Equation 3.2-1 can be symbolically written for junction flow path m as

$$\left(\frac{L}{a}\right)_m \frac{dW_m}{dt} = \Delta P_m + \rho_m g L_m - \rho_L g H_m - \left(\frac{F}{a^2}\right)_m \frac{W_m^2}{2\rho_m} \quad (3.2-3)$$

where,

$$L_m = \sum_n \lambda_{nv} \quad (3.2-4a)$$

$$\left(\frac{F}{a^2}\right)_m = \sum_n \frac{F_n}{a_n^2} = \sum_n \left(\frac{f_n \lambda_n}{D_n} + k_n\right) \frac{1}{a_n^2} \tag{3.2-4b}$$

and

$$\left(\frac{L}{a}\right)_m = \sum_n \frac{\lambda_n}{a_n} \tag{3.2-4c}$$

For the gas-filled line indicated schematically in Figure 3-2a, the gas density is very small compared to that of the liquid and the gas gravity head $\rho_m g L_m$ can be neglected and the submergence $H_m = H_{sub}$. For the liquid-filled line shown in Figure 3-2b, the net gravity head is $L_m = L_1 - L_2$ and the density ρ_m equals that of the average liquid density ρ_L for flow path m. Also, in this case H_m is set equal to zero.

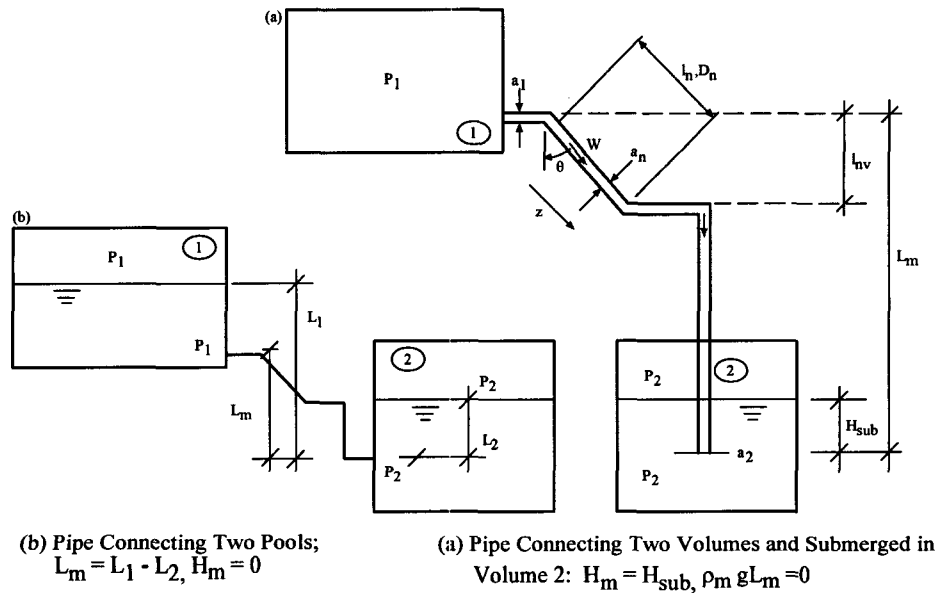


Figure 3-2 Junction Pipes

3.3 Summary

The generic equations governing the flow rates between junctions (Equation 3.2-3), total and component mass conservation (Equations 3.1-1 and 3.1-2), the pressurization rates of volumes (Equation 3.1-7) and the volume internal energy (Equation 3.1-6) were presented in Sections 3.1 and 3.2.

The enthalpies h_o appearing in Equations 3.1-6 and 3.1-7 were *total* specific enthalpies (i.e., the sum of the intrinsic specific enthalpy of the fluid plus its kinetic and potential energies). Consequently, the exact scaling of these would have required separate consideration of specific enthalpy, velocity and elevation scales. Since changes in kinetic and potential energy are very

small or totally negligible, this complication is avoided here and the h_o are replaced by h in the following.

The equations that will be nondimensionalized in subsequent sections are repeated here for convenience:

$$\frac{dM}{dt} - \sum_i W_i = 0 \quad (3.1-1)$$

$$\frac{dM_j}{dt} - \sum_i W_{ij} = 0 \quad (3.1-2)$$

$$\left(\frac{L}{a}\right) \frac{dW}{dt} = \Delta P - \frac{1}{\rho} \left(\frac{F}{a^2}\right) \frac{W^2}{2} + \rho g H^* \quad (3.1-3)$$

$$M \frac{de}{dt} = -P \frac{dV}{dt} + \sum_k \mathcal{E}_k + \sum_i W_i (h_{o,i} - h) + \frac{P}{\rho} \sum_i W_i \quad (3.1-6)$$

$$V f_2 \frac{dP}{dt} = \sum_i [W_i (h_{o,i} - h)] + \sum_i W_i P^* v \sum_k \mathcal{E}_k - P^* \frac{dV}{dt} - V \sum_j \left[f_{1,j} \frac{dy_j}{dt} \right] \quad (3.1-7)$$

$$\rho_g \frac{d\alpha}{dt} = \frac{1}{V} \sum_i W_g + \frac{\sum_i (h_\lambda - h_f) W_\lambda}{V h_{fg}} + \frac{\mathcal{E}}{V} + \frac{\psi}{h_{fg}} \frac{dP}{dt} \quad (3.1-9)$$

$$\frac{dM_1}{dt} = - \sum_k \frac{\mathcal{E}_k}{h_{fg}} + \sum_i W_{1,i} + \sum_i \frac{\Delta h_{sub} W_{1,i}}{h_{fg}} - \frac{1}{h_{fg}} \left[V_{RPV} (1 - \rho_g h'_g) + M_1 \left(\frac{\rho_g}{\rho_1} h'_g - h'_f \right) \right] \frac{dP_R}{dt} \quad (3.1-11)$$

* The hydrostatic head and submergence terms are of the same form and have been combined into one generic term, $\rho g H$.

4.0 SCALING FOR TEST DESIGN

The general scaling criteria applicable to the ESBWR System with its various subsystems and components and their counterparts in the related tests under consideration are derived in this section by a top-down approach. General scaling criteria have been derived by several authors ([4-1], [4-2], [4-3], [4-4]). Generally, these are not specific to the combined thermodynamic and thermal-hydraulic phenomena taking place inside containments and therefore are not directly applicable here. To arrive at general scaling criteria applicable to the ESBWR System, the controlling processes in generic subsystems having the essential characteristics of classes of ESBWR systems (e.g., containment volumes, pipes, etc.) are considered. These lead to generic governing equations for the rate of pressurization of volumes (the "pressure rate equations") and for the flow rates between volumes (the "flow rate equations"). These equations are cast in nondimensional form and various nondimensional groups controlling component or system behavior appear. This has been summarized previously in references 3-1 and 4-5.

The ESBWR System consists of a number of volumes (RPV, DW, SC, etc.) connected via junctions (i.e., openings, piping, vents, heat exchanging equipment such as the ICS and PCCS condensers, etc.). Mass and energy transfers take place between these volumes through their junctions. Heat may also be exchanged by conduction with the structures. These exchanges lead to changes in the thermodynamic condition of the various volumes; this, in particular leads to changes of the volume pressures. The junction flows (flows between volumes) are driven by the pressure differences between volumes. Thus, the thermodynamic behavior of the system (essentially, its pressure history) is linked to its thermal-hydraulic behavior (the flows of mass and energy between volumes). Proper global scaling of these processes is important for the ESBWR-related tests considered here and the topic addressed in this section.

Global scaling is based on the mathematical formulations of the basic physical principles which govern top-down phenomena. Dependent variables like pressure, velocity, mass flow rates, and enthalpies are normalized with respect to either their initial values, or other limiting values, which cause the normalized variables to have an order of magnitude unity; that is, $O(1)$. Only quantities which can be controlled in an experiment are chosen for the normalizing values. The normalizing time scale for top-down phenomena is determined for each LOCA phase; namely, Blowdown, GDCS transition, reflood and PCCS.

Prototypical fluids under prototypical thermodynamic conditions were used in all the ESBWR-related tests. The fact that the fluids are expected (by design and operation of the test facilities) to be in similar states in the prototype and the models, will be used to simplify the following analyses.

4.1 Top down Scaling

These equations will be nondimensionalized using the following reference quantities (denoted by the subscript r):

- For time: t_r
- For volume: V_r
- For mass flow rates: W_r

- For heat addition: \dot{Q}_r
- For densities: ρ_r
- For pressure, a reference pressure difference: ΔP_r
- For properties involving vapor mass function: Ψ_r
- For enthalpies and internal energies, a reference specific enthalpy difference: Δh_r

To derive the general scaling criteria, the equations will be nondimensionalized by dividing the dimensional variables z by the reference values z_r above; this produces the nondimensional variables z^+ :

$$z^+ \equiv \frac{z}{z_r} \quad (4.1-1)$$

In particular, note that:

$$h_{o,i} - h_o \approx h_i - h = h_i^+ \Delta h_r \quad (4.1-2)$$

where h^+ denotes a nondimensional enthalpy difference for flow i (enthalpy of stream entering h_i , minus average volume enthalpy, h).

Also

$$f_{1,j} = f_{1,j}^+ \frac{\rho_r \Delta h_r}{y_{j,r}} \quad (4.1-3)$$

and

$$f_2 = f_2^+ \rho_r \frac{\Delta h_r}{\Delta P_r} \quad (4.1-4)$$

The details of the derivations can be found in Appendices A and B of Ref [3-1]. The resulting nondimensional equations are:

Conservation Equations:

$$\frac{d}{dt^+} (V^+ e^+) - \Pi_t \sum_i W_i^+ = 0 \quad (4.1-5)$$

$$\frac{d}{dt^+} (V^+ \rho_j^+) - \Pi_{t,j} \sum_i W_i^+ y_{i,j}^+ = 0 \quad (4.1-6)$$

Momentum Equation:

$$\Pi_{in} \frac{dW^+}{dt^+} = \Pi_{pd} \Delta P^+ - \Pi_{loss} \frac{W^{+2}}{\rho^+} - \Pi_h \rho^+ H^+ \quad (4.1-7)$$

Energy Equation:

$$\begin{aligned}
 V^+ \rho^+ \frac{de^+}{dt^+} = & -\frac{1}{\Pi_{hp}} \rho^+ \frac{dV^+}{dt^+} + \sum_k \Pi_t \Pi_{pch} \mathcal{E}_k^+ \\
 & + \Pi_t \sum_i W_i^+ h_i^+ + \frac{\Pi_t P^+}{\Pi_{hp} \rho^+} \sum_i W_i^+
 \end{aligned}
 \tag{4.1-8}$$

Pressure Rate Equation:

$$\frac{dP^+}{dt^+} = \frac{1}{V^+ f_2^+} \left\{ \Pi_t \sum_i W_i^+ h_i^+ + \frac{\Pi_t P^{**}}{\Pi_{hp} \rho^+} \sum_i W_i^+ + \sum_k \Pi_t \Pi_{pch} \mathcal{E}_k^+ - \frac{1}{\Pi_{hp}} P^{**} \frac{dV^+}{dt^+} - V^+ \sum_j f_{1,j}^+ \frac{dy_j^+}{dt^+} \right\}
 \tag{4.1-9}$$

Vapor Fraction Equation:

$$\begin{aligned}
 \rho_g^+ \frac{d\alpha}{dt^+} = & \Pi_t \sum_i W_{g,i}^+ + \Pi_t \frac{\sum_i h_{sub,i}^+ W_{\lambda,i}^+}{h_{fg}^+} + \sum_k \Pi_t \Pi_{pch} \frac{\mathcal{E}_k^+}{h_{fg}^+} \\
 & + \frac{\Pi_\psi}{\Pi_{hp}} \psi^+ \frac{dP^+}{dt^+}
 \end{aligned}
 \tag{4.1-10}$$

The Π groups which appear above are defined below:

In the conservation equations:

- The nondimensional time numbers for total flow;

$$\Pi_t \equiv \frac{t_r}{V_r \rho_r / W_r}
 \tag{4.1-11}$$

- and for component j,

$$\Pi_{t,j} \equiv \frac{t_r}{\rho_r V_r / W_r y_{r,j}}
 \tag{4.1-12}$$

In the Momentum Equation:

- The inertial pressure drop number

$$\Pi_{in} \equiv \frac{W_r \left(\frac{L}{a} \right)_r}{\Delta P_r t_r}
 \tag{4.1-13}$$

- The pressure difference number,

$$\Pi_{pd} \equiv \frac{\Delta P_o}{\Delta P_r} \quad (4.1-14)$$

- The pressure loss number,

$$\Pi_{loss} \equiv \frac{W_r^2 \left(\frac{F}{a^2} \right)_r}{2\Delta P_r \rho_r} \quad (4.1-15)$$

- The submergence or hydrostatic level difference number,*

$$\Pi_h \equiv \frac{\rho_r g H_r}{\Delta P_r} \quad (4.1-16)$$

In the Energy and Pressure Rate Equations:

- The enthalpy-pressure number,

$$\Pi_{hp} \equiv \frac{\Delta h_r}{\Delta P_r / \rho_r} \quad (4.1-17)$$

- The phase change number,

$$\Pi_{pch} \equiv \frac{\mathcal{Q}_r}{W_r \Delta h_r} \quad (4.1-18)$$

In the Vapor Fraction Equation:

- The flashing number,

$$\Pi_\psi = \psi_r \quad (4.1-19)$$

- The reference component fraction scales $y_{j,r}$. Considering the fact that the $y_{j,r}$ must be conserved, there is no need to consider $\Pi_{t,j}$. The time number Π_t suffices, since $\Pi_{t,j} = \Pi_t / y_{j,r}$. We are thus left with the following eight Π numbers to match between prototype and model:

$$\Pi_t, \Pi_{in}, \Pi_{pd}, \Pi_{loss}, \Pi_{sub}, \Pi_{hp}, \Pi_{pch} \text{ and } \Pi_\psi$$

4.2 Phase Changes at Interfaces

The phase changes at interfaces involve the latent heat of vaporization and the interfacial mass flow rates and mass fluxes. The reference enthalpy scale Δh_r used above can, in principle, be

* A separate hydrostatic level difference number Π_{hyd} is used later, using a level difference in place of the submergence.

selected arbitrarily. A ¹⁰rational definition for Δh_r arises, however, when phase changes at interfaces are scaled. In this case, the natural choice is $\Delta h_r = h_{fg,r}$, the reference latent heat of vaporization.

Although it is generally difficult to scale exactly phase changes taking place by condensation on structures and walls it is relatively straightforward to scale phase changes at the free pool surfaces. The flow rates due to phase change at the surface of a pool are given by the product of the pool surface area A_{LG} times the mass flux due to phase change \dot{m}_{LG} . The latter, in general, ¹¹depends on the fluid conditions on both sides of the interface (P, T, partial densities of constituents ρ_j) and on hydrodynamic parameters controlling mass transfer (i.e., the Grashoff, Reynolds and Prandtl numbers of the fluids). The hydrodynamic dependence is considered in the bottom-up analysis of Section 7.6. Here we derive the scaling of the surface areas.

The vapor flow rate due to vaporization

$$W_{LG} = A_{LG} \dot{m}_{LG} \quad (4.1-20)$$

must scale the same way as the other flow rates in the system. Assuming that with prototypical fluids and well scaled local conditions at the interface, the phase-change mass fluxes \dot{m}_{LG} in the prototype and the model are identical, one concludes that the pool areas A_{LG} must scale like the flow rates.

4.3 General Scaling Criteria

The nondimensional numbers identified above will now be used to derive general scaling criteria for the experimental facilities.

The analysis of this section considers a single individual flow path and a single volume and derives the general scaling laws applicable to these. These general criteria are applied then to each flow path and volume in the system. The resulting scaling of the entire system, any possible interactions between subsystems¹², and the identification of scaling distortions are considered in Sections 7 and 8.

Although several other choices are also possible, the *system scale* R can be defined as the ratio of prototype to test facility power input:

$$R \equiv \frac{\dot{Q}_{\text{prot}}}{\dot{Q}_{\text{mod}}} = \dot{Q}_R \quad (4.3-1)$$

where the subscript R denotes the ratio between the corresponding scales of prototype and model. For a variable Z :

¹⁰ RAI 265

¹¹ RAI 266

¹² Supp. RAI 259 & Supp RAI 286

$$Z_R \equiv \frac{Z_{\text{prot}}}{Z_{\text{mod}}} \quad (4.3-2)$$

Nine nondimensional groups were identified by the analysis of Section 4.1 (Equations 4.1-11 to 4.1-19). In addition, it was shown that the pool surface areas A_{LG} must scale like the flow rates.

By dividing Π_t by $\Pi_{t,j}$, it becomes evident that the reference component fraction scales $y_{j,r}$ must be conserved; with this constraint there is no need to further consider $\Pi_{t,j}$; instead

$$(y_j)_R = 1 \quad (4.3-3)$$

Also, from consideration of the vapor mass equation $(\alpha)_R = 1$.

For a given flow path, the reference ΔP_r scale can be chosen to be the initial driving pressure difference ΔP_0 ; this makes $\Pi_{pd} = 1$. Furthermore, for all of the ESBWR related tests considered here the facilities were designed to have pressure differences and elevations conserved*. This leads to

$$(H)_R = (\Delta P)_R = 1 \quad (4.3-4)$$

and Π_{pd} needs no longer be considered.

Thus, we are left with the following six Π numbers to match between prototype and model components:

$$\Pi_t, \Pi_{in}, \Pi_{loss}, \Pi_h, \Pi_{hp} \text{ and } \Pi_{pch}$$

in addition to

$$(\alpha)_R = (y_j)_R = (\Delta P)_R = (H)_R = 1 \quad (4.3-5)$$

and

$$(A_{LG})_R = W_R \quad (4.3-6)$$

The minimum set of not-yet specified independent reference scales appearing in the remaining Π numbers listed above is

$$t_r, \rho_r, V_r, W_r, \left(\frac{L}{a}\right)_r, \left(\frac{F}{a^2}\right)_r, \Delta h_r \text{ and } \mathcal{E}_r$$

* Other choices may be possible, but are not considered here.

In Section 4.2, it was shown that a ¹³rational choice for Δh_r was

$$\Delta h_r = h_{fg,r} \quad (4.3-7)$$

Thus, where prototypical fluids are used and the test facilities are designed to operate under prototypical thermodynamic conditions,

$$(\Delta h)_R = (h_{fg})_R = \rho_R = 1 \quad (4.3-8)$$

The pressure evolution resulting from the thermodynamics of the system and the pressure drops between volumes must clearly be scaled in an identical fashion. Considering the fact that prototypical fluids are used, this requirement links the properties of the fluid (in particular, the latent heat and the specific volumes of water and steam) to the pressure differences between volumes (and to the submergence depths of vents or water levels), resulting in 1:1 scaling for pressure drops.

The choice of a proper time scale t_r will be discussed in Section 4.6. To arrive at the general scaling criteria, one can specify $\Pi_t = 1$; this leads to the definition of t_r as the volume residence time,

$$t_r = \frac{V_r \rho_r}{W_r} \quad (4.3-9)$$

Having decided to use 1:1 scaling for pressure drops and elevations and prototypical fluids, matching of the submergence of hydrostatic level difference number Π_h , and of the enthalpy-pressure number Π_{hp} is automatically satisfied.

Matching of the phase change number requires that, for prototypical fluids, the ratio \mathcal{Q}/W be preserved. Having already defined $\mathcal{Q}_R = R$, this leads to

$$\mathcal{Q}_R = W_R = (A_{LG})_R = R \quad (4.2-10)$$

Matching of the remaining inertial pressure drop number and frictional pressure loss numbers,

$$\Pi_{in} = \frac{W_r \left(\frac{L}{a} \right)_r}{\Delta P_r t_r} \quad (4.3-11)$$

and

¹³ RAI 267

$$\Pi_{\text{loss}} = \frac{W_r^2 \left(\frac{F}{a^2} \right)_r}{2\Delta P_r \rho_r} \quad (4.3-12)$$

leads to

$$\left(\Pi_{\text{in}} \right)_R = \frac{R \left(\frac{L}{a} \right)_R}{1} = R \left(\frac{L}{a} \right)_R = 1 \quad (4.3-13)$$

and

$$\left(\Pi_{\text{loss}} \right)_R = \frac{R^2 \left(\frac{F}{a^2} \right)_R}{1} = R^2 \left(\frac{F}{a^2} \right)_R = 1 \quad (4.3-14)$$

These two requirements can be satisfied if

$$L_R = F_R = 1 \quad (4.3-15)$$

and

$$a_R = R \quad (4.3-16)$$

Since $W = \rho a u$, u being the flow velocity in a pipe, with $\rho_R = 1$ and $W_R = R$, the requirement $a_R = R$ leads to identical velocities in the prototype and the model. The scaling of the flow velocities is discussed in Section 4.4.

Although it may be relatively easy to have prototypical lengths of piping in the test facilities (i.e., $L_R=1$), the requirement $F_R=1$ is more difficult to match, since the $f l / D$ components of F (Equation 2.1-2a) cannot be matched when $a_R=R$ and $D_R = \sqrt{a_R} = \sqrt{R}$. The practical scaling of the frictional pressure losses is discussed in Section 4.4.

Instead of conserving F_R and a_R separately, for given F it is clearly sufficient to conserve the ratio $(F/a^2)_R$. However, this will lead to a somewhat different scale for a_R and may lead to distortions of $(L/a)_R$. However, for systems such as the ESBWR containment, where inertial effects play a minor role, the distortion of the inertial effects is usually not important.

The vapor mass continuity equation applied to the two-phase region inside the RPV leads to the need to match Π_ψ in addition to Π_t , Π_{hp} and Π_{pch} . Π_ψ is matched by setting $(\alpha)_R = 1$ and using prototypical pressures and thermodynamic conditions in the experiment. The other Π groups have already been discussed and shown to be matched by scaling $Q_R = W_R = A_R = R$ and maintaining $L_R = 1$.

The axial void distribution and level swell are also matched by setting $L_R = 1$ (Section 3.8 of [3-1]). The two-phase level $L_{2\phi}$ is given by

$$L_{2\phi} = \frac{V_f}{(1 - \bar{\alpha})A} \quad (4.3-17)$$

where V_f is the volume below the level. Level swell will be matched by using the scale of $(V_f)_R = A_R = R$ (i.e., $L_R = 1$).

Since the volume scale V_r appears only in the time constant t_r , one could, in principle, conduct tests at a different time scale (not 1:1) by modifying the volume scale ratio V_R . This is possible as long as t_r is *the* controlling time scale, as already discussed in Section 4.1. Accelerated tests can, for instance, be conducted by decreasing V_R or increasing equally the other scales, $\mathcal{G}_R = W_R = (A_{LG})_R$. Conservation of the time scale t_r also implies (in any case) preservation of the ratio V_r/W_r .

4.4 Scaling of the Piping¹⁴

The scaling of the piping is determined by the already defined pressure drop and reference flow rate scales. The relevant Π number is

$$\Pi_{\text{loss}} \equiv \frac{(F/a^2)_r W_r^2}{2\Delta P_r \rho_r} = 1 \quad (4.4-1)$$

The factor F/a^2 (Equation 3.2-4b) depends on both the frictional losses in the pipes (i.e., on the groups $f_n \lambda_n / D_n$) and on the local losses k_n . The latter are generally insensitive to scale. Since the model diameters D_n are smaller, however, the F/a^2 factors of the models tend to be larger. Thus, conservation of Π_{loss} leads to reduced velocities in the models. This is not important, as long as the transit times between volumes are small compared to the volume fill times t_r , and the velocities do not become so low as to introduce new phenomena in the models.¹⁵

In practice, pipe scaling is performed according to the following procedure: the pipe cross-sectional areas in the scaled facilities are oversized for convenience; this leads to somewhat lower flow velocities in the pipes. Thus, considering only the *local losses* (for which the loss coefficients are only weakly dependent on flow velocity or Reynolds number), the total Δp 's in the models would be *lower* than prototypical. On the contrary, *wall friction* in the scaled

facilities is *larger* (due to larger values of the $f\lambda/D$ values produced by the smaller pipe diameters), as it cannot be compensated in general by the decrease in velocity. Usually (and fortunately), the total pressure drops in the piping are dominated by local losses, so that the total ΔP 's in the scaled facilities end up being somewhat smaller. They can therefore be matched by introducing additional losses by local orificing.

¹⁴ RAI 264

¹⁵ RAI 268

The pipe flow areas determined in this fashion result in velocities that do not lead to matching pipe transit times. This is, however, of secondary importance, as already noted.

In summary, matching of the total pressure drops is accomplished by using orifices in conjunction with convenient choices for pipe diameters.

4.5 Compressibility of the Gas Flowing in Pipes

The gases flowing in pipes connecting containment volumes were treated as incompressible; this assumption is justified in this section.

We start from the continuity equation, written for the pipe segment of Figure 3-2,

$$\frac{dM}{dt} = W_1 - W_2 \quad (4.5-1)$$

where W_1 and W_2 are the mass flow rates at Sections 1 and 2, respectively; in general

$$W = A_p \rho u$$

M is the mass contained in the pipe of volume $V_P = A_P L_P$ and average density $\bar{\rho}$. We nondimensionalize Equation 4.5-1 by defining

$$t^+ \equiv \frac{t}{t_{p,r}}$$

and

$$W^+ \equiv \frac{W}{W_r}$$

with

$$W_r = \rho_r A_p u_r$$

and

$$\rho^+ \equiv \frac{\rho}{\rho_r}$$

and a pipe transit time

$$t_{t,r} \equiv \frac{L_p}{u_r}$$

Equation 4.5-1 takes the nondimensional form

$$\frac{t_{tr,r}}{t_{p,r}} \frac{d\bar{\rho}^+}{dt^+} = W_1^+ - W_2^+ \quad (4.5-2)$$

It is evident that if $t_{p,r} \gg t_{tr,r}$ (i.e. rate of change of the average density is small), the mass flow rates at the inlet and the exit of the pipe will be approximately equal, $W_1^+ \approx W_2^+$, or $W_1 \approx W_2$. So clearly, the pipe transit time $t_{tr,r}$ must be compared to the other time constants of the system

4.6 Time Scales

Several time scales appeared during the general scaling considered in this section. These are briefly discussed here.

Volume fill time

This first time constant is related to mass continuity and is the volume fill time¹⁶ for mass flowing into the volume V_r at the mass flow rate W_r [2-1]:

$$t_{m,r} = \frac{V_r \rho_r}{W_r} \quad (4.6-1)$$

The volume fill time t_r is the¹⁷ reference time for subsystems and processes where volume emptying or filling due to mass flows takes place.¹⁸

Pressurization Time Constant

Another time scale comes from the pressure rate equation and is related to the time for a volume to depressurize due to enthalpy flows. For a volume V_r with flow W_r leaving at an enthalpy Δh_r greater than the average enthalpy, the time constant for blowdown is:

$$t_r = \frac{V_r \rho_r}{W_r} \frac{\Delta P_r}{\Delta h_r} \left(\frac{\partial e}{\partial p} \right)_r \quad (4.6-2)$$

This is related to the volume fill time constant by

$$t_r = t_{m,r} \frac{\Delta P_r}{\Delta h_r} \left(\frac{\partial e}{\partial p} \right)_r \quad (4.6-3)$$

This is the natural time constant for subsystems and processes where volume pressurization due to enthalpy flows takes place.

Flashing Time Constant

¹⁶ RAI 270

¹⁷ RAI 271

¹⁸ RAI 263

When a saturated volume depressurizes, there is a time constant associated with the swelling of the liquid region to reach a quasi-steady void fraction:

$$t_{\text{flash},r} = \frac{\rho_{g,r}}{\Gamma_r} \quad (4.6-4)$$

This is the time constant associated with the beginning of a blowdown event such as those at the initiation of the GIST and GIRAFFE/SIT tests.

Inertial Time Constant

Another time scale is needed in scaling the inertial effects in the momentum equation, written in nondimensional form as Equation 4.1-7:

$$\Pi_{\text{in}} \frac{dW^+}{dt^+} = \Pi_{\text{pd}} \Delta P^+ - \Pi_{\text{loss}} \frac{W^{+2}}{\rho^+} - \Pi_{\text{h}} \rho^+ H^+ \quad (4.6-5)$$

where the *inertial pressure drop number*

$$\Pi_{\text{in}} \equiv \frac{W_r \left(\frac{L}{a} \right)_r}{\Delta P_r t_{\text{in},r}}$$

appeared. The inertia time scale is obtained by comparing the inertial Π group, Π_{in} , with the dominant Π group driving the flow on the right hand side of equation 4.6-5 (i.e. either Π_{pd} or Π_{h}). For liquid filled pipes driven by hydrostatic head such as the condenser drain lines this yields

$$\Pi_{\text{in}} \left(= \frac{W_r \left(\frac{L}{a} \right)_r}{\Delta P_r t_{\text{in},r}} \right) = \Pi_{\text{h}} \left(= \frac{\rho_r g_r H_r}{\Delta P_r} \right) \quad (4.6-6)$$

or

$$t_{\text{in},r} = \frac{W_r \left(\frac{L}{a} \right)_r}{\rho_r g_r H_r} \quad (4.6-7)$$

but $W_r = \rho_r a_r u_r$ and $L_r \approx H_r$ so that

$$t_{\text{in},r} = \frac{u_r}{g} \quad (4.6-8)$$

When the process is dominated by a sudden imposed pressure differential, a balance between the inertial and pressure difference terms controls the flow so that:

$$\Pi_{in} \left(= \frac{W_r \left(\frac{L}{a} \right)_r}{\Delta P_r t_{in,r}} \right) = \Pi_{pd} \left(= \frac{\Delta P_o}{\Delta P_r} \right) \quad (4.6-9)$$

This leads to the alternate definition of the inertial time constant:

$$t_{in,r} = \frac{W_r \left(\frac{L}{a} \right)_r}{\Delta P_o} = \frac{\rho_r u_r L_r}{\Delta P_o} = \frac{u_r \rho_r g L_r}{g \Delta P_o} \quad (4.6-10)$$

Thus, the inertial time scale $t_{in,r}$ can be thought of as the time roughly needed to accelerate the fluid from zero to u_r as a result of the dominant driving force.

Pipe Transit Time¹⁹

Finally, a *pipe transit time* was defined in Section 4.5 as

$$t_r \equiv \frac{L_p}{u_r} \quad (4.6-11)$$

Comparison of the Time Scales

The five time scales produced by this analysis (t_r , $t_{m,r}$, $t_{flash,r}$, $t_{in,r}$, and $t_{tr,r}$) scale the rates of pressurization, volume fill, flashing/redistribution, inertial effects, and pipe transfers, respectively. Clearly, the systems considered here are made of large volumes connected by piping of much lesser volumetric capacity. The pressure drops between these volumes are not expected to be dominated by inertial effects. Thus, the inertia and transit times, which are of the same order of magnitude, are much smaller than the volume fill times:

$$t_r \approx t_{m,r} \gg t_{in,r} \approx t_{tr,r} \quad (4.6-12)$$

For this condition, the time behavior of the system will be controlled by the pressurization rates. The pipe transit times and the inertial time scale of the piping ($t_{tr,r}$ and $t_{in,r}$) are much shorter and the overall dynamics of the system will not be controlled by such effects.

¹⁹ RAI 269

A discussion of the non-dimensional reference time (and other) Pi parameters is provided in Section 4.1.

4.7 Specific Frequencies of the Process

Another way of viewing the processes taking place is by considering their specific frequencies which are given as ratios of a transfer intensity to capacity (amount) of the receiving volume [2-1]. In the particular case considered here, two specific frequencies involved are the ratio of heat addition \dot{Q}_r and enthalpy addition $W_r \Delta h_r$ to the heat capacity of the receiving volume $V_r \rho_r \Delta h_r$:

$$\omega_{\dot{Q}_r} \equiv \frac{\dot{Q}_r}{V_r \rho_r \Delta h_r} \quad (4.7-1)$$

and

$$\omega_{\Delta h} \equiv \frac{W_r \Delta h_r}{V_r \rho_r \Delta h_r} \quad (4.7-2)$$

A *residence* or *fill* time t_r has already been defined as

$$t_r = \frac{V_r \rho_r}{W_r} \quad (4.7-3)$$

The product of $\omega_{\dot{Q}_r}$ and t_r results in the phase change number,

$$\omega_{\dot{Q}_r} \cdot t_r = \Pi_{pch} \quad (4.7-4)$$

as expected, while $\omega_{\Delta h} \cdot t_r = 1$; no new nondimensional number is derived.

A third specific frequency is the ratio between the intensity of enthalpy addition $W_r \Delta h_r$ and the "capacity of the volume to absorb work" $V_r \Delta p_r$:

$$\omega_{\Delta p} \equiv \frac{W_r \Delta h_r}{V_r \Delta p_r} \quad (4.7-5)$$

The product of $\omega_{\Delta p}$ with t_r produces, as expected, the enthalpy-pressure number Π_{hp} ,

$$\omega_{\Delta p} \cdot t_r = \Pi_{hp} \quad (4.7-6)$$

Consider now the specific frequency of the transfers of mass in the piping. Again, considering the ratio of an intensity of transfer (the volumetric flow rate) to the (volumetric) capacity of the piping, we obtain

$$\omega_{tr} \equiv \frac{W_r}{\rho_r L_v a_r} = \frac{u_r}{L_v} \quad (4.7-7)$$

where L_v is the equivalent volume-length of the piping. The pipe transit time (already used above) is the inverse of ω_{tr} :

$$t_{tr,r} \equiv \frac{1}{\omega_{tr}} = \frac{L_v}{u_r} \quad (4.7-8)$$

4.8 Summary

The analysis presented in this section has shown that when prototypical fluids under prototypical thermodynamic conditions are used:

Given a system scale R defined as the ratio of power input between model and prototype

$$R \equiv \mathcal{Q}_R \quad (4.8-1)$$

to obtain identical pressure differences and pressure evolution between prototype and model:

- The elevations in the prototype and in the model must be identical, especially the submergence depths of the vents and the water levels in vessels:

$$\Delta P_R = H_R = 1 \quad (4.8-2)$$

- The piping must satisfy the following two relations:

$$\left(\frac{L}{a}\right)_R = \frac{1}{R} \text{ and } \left(\frac{F}{a^2}\right)_R = \frac{1}{R^2} \quad (4.8-3)$$

If $L_R \approx 1$, and F can be chosen in the model so that $F_R \approx 1$, this leads to the scaling of flow areas like

$$a_R = R \quad (4.8-4)$$

If the condition $F_R \approx 1$ cannot be met, then the flow areas can be adjusted to keep

$$\left(\frac{F}{a^2}\right)_R = \frac{1}{R^2} \quad (4.8-5)$$

The factor F/a^2 determining the total pipe losses, can be adjusted by increasing the model pipe diameters and by introducing local losses in the model to match the pressure drops, if necessary.

- The pipe flow areas determined in this fashion result in velocities that do not match the pipe transit and inertial times; usually, the velocities in the model may be smaller than those of the prototype. This is, however, not important as long as the pipe transit and

inertial times are small *compared to the volume* fill times t_f ; the distortion of the inertial characteristics of the system is not important for relatively slow transients.

- The flow rates, heat inputs and horizontal pool areas must be scaled according to the system scale R ,

$$\dot{Q}_R = W_R = (A_{LG})_R = R \quad (4.8-6)$$

- *If*, in addition, the volumes are also scaled with R ,

$$V_R = R \quad (4.8-7)$$

the time scale between model and prototype is 1:1. In this case, we can speak of a vertical *slice* or vertical *section* model of the prototype.

5.0 SYSTEM DESCRIPTIONS

5.1 Introduction

The purpose of this section is to present a summary description of the test facilities that have been used to confirm the design adequacy of the ESBWR response to a LOCA and to qualify the TRACG computer code for the analysis of ESBWR post-LOCA performance. The focus of the tests and the TRACG qualification is the performance of the passive safety systems that maintain core cooling and remove decay heat from the primary system and the containment. The main systems performing these functions are the Gravity-Driven Cooling System (GDSCS), the Isolation Condenser System (ICS), and the Passive Containment Cooling System (PCCS). Although the test facilities described herein were originally designed and built to confirm system performance and qualify the TRACG code for the original SBWR design [5-1], the test data and the TRACG qualification are directly applicable to the ESBWR. This update of the test facility descriptions is provided to keep the present document reasonably self-contained, and to clarify the application of the testing to the larger and higher-power ESBWR. The descriptions provided here are overviews. A full set of references describing details of the various test facilities can be found in the ESBWR TAPD [21-2].

A summary description of the post-LOCA response of the ESBWR with specific emphasis on the passive safety systems that perform the functions of core cooling and decay heat removal is presented in Section 5.2. In subsequent sections, the test facilities used to confirm ESBWR system performance and provide data for TRACG qualification are described. These descriptions include the major considerations that governed the design and scaling of the test facilities for the original SBWR and the scaling adjustments implied by the application of the test results to the ESBWR. The design of the experimental facilities and the conduct of the various tests were guided by consideration of the proper modeling and simulation of the key phenomena governing the performance of the passive safety systems. The implications of the scaling adjustments for the ESBWR are minimized by the fact that all of the tests were performed at prototypical temperature and pressure and with prototypical or near-prototypical elevations and elevation differences. These are the key variables and parameters governing the performance of the passive safety systems.

The test facilities included in the following discussion are listed in Table 5-1. They include the GIST and GIRAFFE/SIT facilities for integral systems testing of GDSCS performance (core cooling); the PANDA and GIRAFFE/He facilities for integral systems performance of the PCCS and ICS (long-term containment heat removal); the PANTHERS passive containment condenser (PCC) and isolation condenser (IC) component tests; and the UCB and MIT laboratory tests that supported the development of correlations for PCC and IC condensation heat transfer that have been incorporated in TRACG. The PANDA test facility is described in greater detail than the others because it was specifically modified to include a containment design innovation of the ESBWR, and was subsequently used to perform a new series of long-term post-LOCA containment cooling tests, similar to the original SBWR test matrix. These tests provided further confirmation of the design adequacy of the ESBWR and enhanced the qualification basis for the TRACG code [5-2].

The integral test²⁰ facilities were designed according to the general scaling criteria summarized in Section 4.8. In addition, each test has some unique variations to these criteria either to take advantage of eliminating unnecessary cost or to enhance the capability of the facility. The specifics of these variations are²¹ covered in subsequent sections.

To facilitate a common understanding of the use of the SBWR and ESBWR test programs for confirmation of ESBWR design adequacy and for TRACG qualification, the following convention has been adopted for the discussion of the test facilities: In the majority of cases, where a characteristic of the test facility was originally designed to represent the SBWR but is equally representative of the ESBWR, the notation E/SBWR will be used. In those cases where a facility characteristic is uniquely associated with the SBWR or (in the case of the modified PANDA facility) the ESBWR, those separate notations will be used.

5.2 Post-LOCA Response of the ESBWR

In the event of a break in the primary system, the ESBWR uses passive safety systems to cool the core and remove decay heat from the primary system and the containment. The main systems performing these functions are the GDCS, the ICS and the PCCS. Emergency core cooling water is provided by the GDCS. The GDCS consists of three water pools situated above the top of the core, from which makeup coolant flows by gravity to replenish the coolant lost from the reactor pressure vessel (RPV). Operation of the GDCS requires depressurization of the RPV and the ESBWR is equipped with an Automatic Depressurization System (ADS) that performs this function. The depressurization of the BWR primary system and the RPV phenomena associated with the early phase of a blowdown have been studied extensively for established BWR designs. A comprehensive set of test programs investigating these phenomena has been used for TRACG qualification [5-3]. The containment loads during early blowdown have also been extensively investigated and are evaluated by established procedures that relate them to the thermal-hydraulic conditions in the containment [5-4].

Decay heat removal from the ESBWR primary system is performed by the ICS, which consists of four Isolation Condensers (ICs) located in a set of interconnected IC and PCC pools high in the reactor building. When redundant condensate return valves are opened, steam from the RPV flows into the tubes of the ICs, condenses, and returns to the RPV, removing stored energy to the atmosphere. The behavior of the IC is well understood because ICs have been in operation for many years in older BWRs. Decay heat is removed from the drywell (DW) by the PCCS, which employs four PCC condensers located in the same set of interconnected pool compartments as the ICs. The PCC condenser tubes are permanently open to the DW so that no operator action is required to actuate the PCCS. A mixture of steam and a time-varying fraction of noncondensable gases (principally, nitrogen, which is used to inert the containment environment) enters the PCC condensers. The steam condenses and the noncondensable gases are vented to the Suppression Chamber (SC) beneath the surface of the suppression pool (SP).

In addition to the PCC vents, the DW volume is connected directly to the SP via the main pressure suppression vents. The PCCS is designed to minimize flow through the main vents by locating the PCCS vent discharges at a higher elevation in the SP than the uppermost main vent

²⁰RAI 275

²¹RAI 276

discharges. This ensures that containment cooling can be accomplished by passive means and, specifically, eliminates the need for the SP to have an active safety-grade cooling system. The PCCS is designed to condense essentially all of the steam produced by decay heat and to vent any noncondensable gases and residual steam to the SP at a temperature close to saturation at atmospheric pressure (i.e., $\sim 100^{\circ}\text{C}$). There is sufficient boiloff water inventory in the IC/PCC pools to ensure coverage of no less than 50% of the length of the condenser tubes for 72 hours from the start of the LOCA. This ensures that the PCCS has sufficient capacity to remove the decay heat throughout this time period with no replacement of pool inventory.

5.3 GIST

GE conducted the GDCS Integrated Systems Test (GIST) series in San Jose, California in 1988. The objectives and conditions for the 24 GIST tests are described in detail in the ESBWR TAPD [2-1]. Proof of the technical feasibility of the GDCS concept was a major test objective. Additionally, test data were obtained for E/SBWR TRACG qualification during the late blowdown and GDCS periods of LOCA transients.

5.3.1 Facility Description

The GIST facility (Figure 5-1) was a section-scaled simulation of the 1987 SBWR design configuration. The major difference between the 1987 SBWR design and the E/SBWR design is that the early design used a single pool of water to provide both the containment pressure suppression function and the water source for core cooling. The E/SBWR replaced this concept with separate GDCS and pressure suppression pools. The E/SBWR also increased the capacity of the GDCS injection lines and reconfigured the ADS relative to what was simulated in GIST. A prior evaluation of these differences concluded that the key GIST parameters (RPV and GDCS water levels and containment pressure) were either conservative or representative with respect to the final E/SBWR design [5-5].

GIST used cylindrical vessels to represent the regional volumes of the E/SBWR. Relative to the E/SBWR, the facility had a 1:1 vertical scale. The horizontal area scale of the RPV and containment volumes relative to the SBWR was 1:508. This translates to an ESBWR area/volume scale of approximately 1:1000. The same SBWR scaling (1:508) and ESBWR adjustment ($\sim 1:1000$) applies to the GIST simulation of RPV decay power.

All significant plant features that could affect the performance of the GDCS were included in the design. GDCS activation is determined by the containment pressure in conjunction with the GDCS pool water level. Consequently, scaled representations of the DW and SC were part of the facility. The piping included simulations of the Automatic Depressurization System (ADS), the GDCS injection lines, and the broken line from the RPV. Capability was provided to simulate conditions at the break location for a range of break types [5-5]. The GIST scaling produced data at real time and at prototypical pressures and temperatures.

5.3.2 Initial Conditions and Test Control

The initial conditions for the GIST tests were determined from TRACG simulations of the initial blowdown behavior of the SBWR from 7 MPa. The facility was first depressurized from 1.03 MPa to 0.79 MPa by venting to the atmosphere. This initial depressurization, which was accomplished over a period of 30 to 50 seconds, created representative thermal-hydraulic

conditions in the RPV²² as it entered the later stages of the depressurization transient (Figure 5-2). The important RPV conditions are the water level and the void fraction distribution. The vessels representing the containment were pressurized and preheated to the TRACG calculated pressures and temperatures at the time the RPV pressure reached 0.79 MPa. The DW was purged of air with steam to simulate the air carryover to the SC during the initial blowdown. Initial SP water temperatures ranged from 42 to 69°C and encompassed the expected conditions in the E/SBWR. The initial RPV water level was increased to compensate for the inability of the GIST facility to represent the creation and sustenance of voids in the lower plenum by stored energy release from the walls of the RPV.²³

When the RPV reached a pressure of 0.79 MPa, the blowdown flows through both the broken line and the ADS lines were switched from the atmosphere to the containment. With further depressurization of the RPV, the head of water in the GDCS eventually became sufficient to overcome the RPV pressure and open the GDCS check valves. This allowed GDCS flow to enter and reflood the vessel.

5.4 GIRAFFE

The GIRAFFE test facility was a full-height, reduced volume, integral system test facility built and operated by Toshiba at its Kawasaki City, Japan site. Test data were obtained for E/SBWR TRACG qualification during the late blowdown/early GDCS phase for liquid-line breaks (GIRAFFE/Systems Interaction Test (SIT)) and during the long-term post-LOCA containment cooling period (GIRAFFE/Helium Test). An important objective of the GIRAFFE/SIT series was confirmation of GDCS performance while operating in parallel with the ICS and PCCS. As the name suggests, the main objective of the GIRAFFE/Helium series was to investigate PCCS performance in the presence of helium as a stand-in for a lighter-than-steam noncondensable gas.

5.4.1 Facility Description

A schematic of the GIRAFFE facility, configured for the SIT series, is shown in Figure 5-3. (This figure minus the ICS and the piping used to simulate liquid line breaks is equally applicable to the GIRAFFE/Helium facility configuration.) Separate vessels represented the RPV, DW, SC, GDCS pools, and the pools that provide secondary-side heat removal for both the ICS and PCCS condensers. The scaled GIRAFFE heater power was based on the E/SBWR decay heat curve, adjusted to compensate for stored energy release in the prototype RPV, which was otherwise not scaled by the GIRAFFE facility. Elevations and submergences scaled the E/SBWR at 1:1 with minor variations as discussed below. Volume scaling relative to the SBWR was nominally 1:300 for the RPV and 1:400 for the other vessels. These ratios correspond to approximately 1:600 for the ESBWR RPV and 1:800 for the other ESBWR vessels. Similarly, power scaling was 1:400 for the SBWR, and approximately 1:800 for the ESBWR. The same scaling ratios applied to the mass flow rates. Prototypical pressures, temperatures and pressure drops were preserved.

The ESBWR RPV was simulated in full height from the bottom of the core to the main steam line (MSL) and the RPV-to-PCC and RPV-to-GDCS pool elevation differences were preserved.

²²RAI 277

²³RAI 278

The RPV regions below the bottom of the core and above the MSL were shortened but the overall volume of the RPV was preserved. The DW was approximately full-height, with some shortening of the regions above and below the region representing the E/SBWR annular DW (i.e., the portion of the DW surrounding the RPV). The variation of DW volume with height in the annular region was preserved so that the DW LOCA water level transient following a liquid break was similar to that expected in the E/SBWR. The lower drywell volume in the GIRAFFE facility was capable of retaining noncondensable gases and/or water as can occur in the E/SBWR.

The GIRAFFE scaling preserved the full height of the E/SBWR SC and GDCS. The configuration of the piping interconnecting the vessels corresponded to the E/SBWR with the exception of the line between the GDCS pool airspace and the DW (see ²⁴'ESBWR Design Description', NEDC-33084P, Rev 1, August 2003 for a discussion of the GDCS to containment connection in the ESBWR). A vacuum breaker line connected the upper DW to the SC gas space as in the E/SBWR. The E/SBWR elevations of the three LOCA vent line discharge points and the PCC vent line discharge point were preserved. All lines interconnecting the vessels were sized and orificed to produce prototypical pressure drops at scaled mass flow rates.

The GIRAFFE PCC condenser was a three-tube representation of the E/SBWR PCCS condensers. The GIRAFFE PCC tubes were thicker than the E/SBWR tubes and, in consequence, on a purely geometric basis, the GIRAFFE PCCS scaling was about 1:690 for the SBWR. However, earlier steady-state GIRAFFE testing indicated that pure numeric and geometric scaling of the tubes relative to the prototype underestimated the heat removal capacity of the GIRAFFE condenser. It was concluded that significant heat transfer was occurring through the non-prototypical GIRAFFE headers. The net effect was to scale the PCCS at 1:430 for the SBWR (i.e., approximately 1:800 for the ESBWR), which, coincidentally, is consistent with the overall system scale. The three GIRAFFE condenser tubes were spaced so as to maintain a representative secondary-side per-tube cross-sectional flow area. A chimney surrounding the condenser unit was used to simulate the expected predominant circulation pattern in the E/SBWR condenser pools.

5.4.2 GIRAFFE/SIT Tests

The parameters of primary interest for the GIRAFFE/SIT tests were those associated with the RPV blowdown and transient water level and related systems interactions. Systems of primary interest in this regard are the GDCS, ICS, PCCS and the systems controlling RPV depressurization. The containment pressure response is important because the pressure adds to the driving head for the GDCS injection flow and impacts the blowdown flow rate once it is no longer choked. The important parameters for maintaining the correct drywell pressure are the hydraulic resistances and discharge submergences of the flow paths between the DW and the SC. These parameters were accurately represented in the GIRAFFE facility

5.4.3 GIRAFFE/Helium Tests

The primary purpose of the GIRAFFE/Helium tests was to demonstrate the operation of the Passive Containment Cooling System (PCCS) in post-accident containment environments including both lighter and heavier-than-steam noncondensable gases. The test matrix included

²⁴ RAI 279

tests in which the DW was initially charged with nitrogen and/or helium and tests with helium addition over time to simulate the transient release of a lighter-than-steam noncondensable gas. These tests demonstrated E/SBWR containment thermal-hydraulic performance and PCCS heat removal in a wide range of potential containment accident environments. In addition, they provided data for TRACG qualification for prediction of containment response in the presence of lighter-than-steam noncondensable gases.

5.5 PANDA

The large-scale PANDA integral systems test facility at the Paul Scherrer Institute (PSI) in Switzerland provided a comprehensive set of test data for confirmation of the performance of E/SBWR passive safety systems for long-term post-LOCA containment cooling and for TRACG qualification. The issues addressed by PANDA testing included parallel operation of multiple PCC loops, parallel operation of the ICS and PCCS, DW-to-WW bypass leakage and the delayed release of noncondensable gas in the DW. The PANDA scaling of elevations, gravity heads and submergences was 1:1 for the E/SBWR. Volume/power scaling was 1:25 for the SBWR, which corresponds to approximately 1:50 for the ESBWR. The experiments were conducted under prototypical pressure and temperature conditions for the phase of the accident under considered.

Two sets of PANDA transient tests contribute to the ESBWR qualification basis. The first set (the "M-series") was performed in support of the original SBWR design. From the standpoint of PCCS performance and TRACG qualification, the M-series data are also applicable to the ESBWR. The second and more recent set of tests (the "P-series") was performed explicitly in support of the ESBWR, as confirmatory tests. Prior to the execution of the P-series tests, the PANDA facility was reconfigured to incorporate an ESBWR design change that connected the airspace of the GDCS pool to the WW instead of the DW as in the SBWR. This change effectively increases the ratio of WW to DW volume and reduces the long-term containment pressure by providing a larger repository for the initial DW inventory of noncondensable gas. A detailed comparison between the P-series test data and TRACG test predictions is provided in Reference 5-2.

5.5.1 Facility Description

A schematic of the PANDA test facility is shown in Figure 5-4. Early in the conceptual design phase, it was concluded that it was not practical to preserve exact geometric similarity between the prototype containment volumes and the experimental facility. However, it is expected that multidimensional phenomena such as mixing of gases within large volumes and natural circulation between volumes will depend on the geometry of the containment building. The approach followed was to allow multidimensional effects to take place by representing both the DW and the SC with two vessels, and by providing a range of well-controlled boundary conditions (e.g., RPV steam flow to one or both DW vessels) to study various system scenarios and alternative accident paths. In this way, the various phenomena could be studied under well-defined conditions and a behavior envelope of the system established. A corollary advantage of this approach is that carefully conducted parametric experiments provide the most useful data for code qualification.

As described above, the PANDA DW and SC are each represented by two interconnected cylindrical vessels (Figure 5-4). The RPV and GDCS pool were each represented by a single

cylindrical vessel. The RPV contains an electrical heat source with a 1.5-MW capacity. There are three PCCS condensers representing the four units in the ESBWR. The PCC condensers are open to the two DW vessels, as shown in Figure 5-4. The fact that there are two PCC units connected to DW2 and one unit to DW1 produces a degree of asymmetric behavior between the two DWs even when they receive equal flow from the RPV. There is a single ICS condenser representing, in terms of heat removal capacity, approximately two of the four ESBWR units. The ICS is activated by opening the valve in the condensate return line to the RPV. The facility is heavily instrumented with approximately 560 sensors for temperature, pressure, pressure difference, level or void fraction, flow rate, gas concentration, electrical power, and conductivity (presence of phase) measurements.²⁵

5.5.1.1 Vessels

Figure 5-5 shows the geometrical arrangement of PANDA in comparison to the E/SBWR and the relative elevations of the two systems. All the E/SBWR RPV elevations are represented except those below the top of the active fuel (TAF). The top of the PANDA RPV electric heaters is placed at the TAF location but the heaters are only about 1/2 the height of the E/SBWR core. The RPV liquid inventory above the bottom of the active fuel (BAF) is scaled according to the system scale. The RPV liquid inventory below BAF was eliminated because it is essentially inactive during the long-term cooling phase of the post-LOCA transient and is not required for the correct simulation of any gravity heads. The liquid volume between mid-core and BAF was included in the scaled PANDA RPV volume by a small adjustment of the vessel diameter. Eliminating and redistributing the water volume below mid-core and modifying the length of the heater elements does not significantly influence any natural circulation paths. The PANDA RPV includes a downcomer and a riser above the heater rods. The flow areas in the downcomer, the riser, and the core are scaled according to the system scale. The diameter of the PANDA riser is close to the hydraulic diameter of one partition of the E/SBWR riser. The PANDA facility did not include a steam separator and dryer because liquid entrainment and RPV-to-DW pressure drop are insignificant for the portion of the post-LOCA transient simulated by PANDA.

A portion of the lower SP was eliminated in PANDA to reduce vessel size. This is acceptable because the water at the bottom of the pool does not participate in the system thermal-hydraulic response during the long-term cooling phase of a LOCA. The important phenomena take place above the submergence depth of the top row of LOCA vents and, for the most part, above the discharge point for the PCCS vents. There is sufficient water below the main vent discharge in PANDA (~1.6 m) to ensure prototypical mixing during the LOCA period simulated. The effect of deeper mixing during the blowdown phase in the E/SBWR is represented by the setting of the test initial conditions. There is sufficient clearance between the PCC vent discharge elevation and the bottom of the SC vessel (~2 m) to ensure prototypical venting of noncondensibles and residual steam. Effects such as the convection of water to the bottom of the vessel by cold plumes running down the walls are of minor importance [5-6].

From Figure 5-5, it can be seen that the region of the DW surrounding the RPV (the annular DW) and the region below the RPV skirt (the lower DW) were not explicitly represented in PANDA. (The volume of the annular region was included in the scaled volume of the PANDA DW.) This was judged to be an acceptable simplification of the test facility because the only

²⁵RAI 272

potentially important phenomenon taking place in these regions is retention and subsequent upward convection of a portion of the initial DW noncondensible inventory. This effect is considered in the test matrix by including tests with a delayed injection of noncondensible gas into the DW.

The PANDA GDCS vessel is roughly a factor of two smaller in relation to the E/SBWR than the system scale applied to the other vessel volumes. This is acceptable because the injection of the initial GDCS inventory to the RPV has been completed prior to the start of the portion of the LOCA transient simulated by PANDA. The GDCS volume is sufficient to hold the water inventory remaining at one hour from the start of the LOCA. During the subsequent long-term containment cooling phase, the main function of the GDCS is to provide a return path for the PCCS and ICS condensate to the RPV. Both the original M-series and the more recent P-series test matrices did, however, include one test that picked up the LOCA transient at a time when the GDCS pool is still draining its initial inventory to the RPV. It was recognized that the subscaled GDCS volume imposed a limitation on the degree to which these "early-start" tests could be expected to produce prototypical behavior. The early-start tests did, nonetheless, provide valuable information for TRACG qualification and assessment of PCCS performance with systems interactions suggestive of E/SBWR behavior during the transition from GDCS injection to PCCS operation in a noncondensible environment.

A final PANDA volumetric scaling compromise was the inventory of the PCCS/ICS pools. In the ESBWR, the boiloff volume is sufficient to maintain coverage of at least 50% of the condenser tube length for a period of 72 hours from the start of the LOCA. In PANDA, 50% of the tube length is exposed in about 18 hours from the start of a test with scaled prototypical decay heat. However, with the exception of one test that was run specifically to investigate the effect of pool boildown on PCCS performance, none of the PANDA tests was run long enough for pool boildown to play a role in the simulation.

5.5.1.2 PCCS/ICS

The PANDA facility includes a PCCS with three PCC loops and an ICS with one IC loop. For the SBWR, the three PCC loops corresponded to the three loops in the prototype PCCS, and the one IC loop represented one of the three IC loops in the prototype ICS. A key factor that led to the original PANDA SBWR system scale of 1:25 was the objective of simulating prototypical PCC and IC secondary-side behavior. The PANDA condensers are, effectively, vertical "slices" from the prototype condensers (Figure 5-6) and are fully prototypical with respect to tube height, pitch, diameter, and wall thickness. With the inclusion of baffles that prevent non-prototypical flow into the bundle in the direction of the header axis, the circulation of the secondary-side water in a plane perpendicular to the axis of the headers is similar to that in the prototype condenser pools. Scaling is determined by the number of tubes included in the slice. The fundamental scaling consideration was to include enough tubes to have a good overall representation of secondary-side heat transfer while not enlarging the overall facility beyond practical limits. This led to the choice of five rows of tubes (i.e., twenty tubes in total).

For the SBWR, which had three PCC units with approximately 500 tubes per unit, the choice of twenty tubes for the PANDA condensers dictated a system scale of 1:25. For the ESBWR, the individual PCC units have about one-third more tubes than the SBWR units and the prototype

PCCS has four PCC loops. The combination of these two factors results in a PANDA scale of 1:50 for the ESBWR PCCS. At a scale of 1:50, the one IC loop in PANDA represents approximately two of the four IC loops in the ESBWR. The scaling of the PANDA vessel volumes for the ESBWR adheres to the 1:50 ratio less stringently than the original 1:25 scaling for the SBWR but, on an overall basis, the characterization of PANDA ESBWR scaling as 1:50 is a good approximation.

5.5.1.3 Flow Paths Between Vessels

The PANDA piping is scaled according to the system scale. The pipe diameters were calculated to match the frictional and form losses of the E/SBWR at the scaled mass flow rates and the resulting pipe diameters were rounded to the next larger standard diameter. This process was facilitated by the fact that the actual pressure drops are dominated by form losses that depend weakly on flow velocity. The lines were provided with orifice plates that were used to adjust the pressure losses following calibration testing. The PANDA main steam lines (one to each DW from the RPV) were scaled to represent the combination of the E/SBWR MSLs and DPVs. To investigate asymmetric DW conditions, all of the RPV steam flow could be directed through one of the steam lines to one DW. The PANDA main vents have a cross-sectional area smaller than the one dictated by the system scale but the gas velocities in the main vents during the phase of the LOCA simulated in PANDA are small enough to produce negligible frictional loss. The vacuum breakers, which provide the flow path for potential redistribution of noncondensable gas between the SC and the DW, were simulated by control valves that were programmed to reproduce the characteristics of the E/SBWR vacuum breakers.

5.5.1.4 Vessel Heat Capacity and Heat Losses

The simulation of the heat capacity of the various SBWR structures was contemplated during the original design phase of the PANDA facility. The PANDA vessels have thin walls with limited heat capacity. The insertion of heat capacity "slabs" in the vessels to match the heat capacity of the E/SBWR structures, and the use of layers of different materials to simulate the response time of the prototype walls were considered. In the end, these concepts were not implemented because it was estimated that energy absorption in the E/SBWR boundary structures during the long-term containment cooling period was of the same order of magnitude as the PANDA facility heat losses. Facility characterization tests showed that heat losses were between 3% and 6.5% of the scaled decay heat [5-7]. The heat loss data were used to calibrate the TRACG model of the PANDA facility.²⁶

5.5.2 Establishment of Test Initial Conditions

The initial conditions for most of the PANDA M-series and P-series tests were representative of the state of the E/SBWR at the start of the long-term containment cooling period following a postulated guillotine rupture of a main steam line. Conditions at this time in the LOCA transient were derived from E/SBWR TRACG calculations. Unique sets of initial conditions were specified for tests simulating an earlier start in the LOCA transient or extreme conditions designed to challenge the performance of the PCCS (e.g., tests initiated with the DW filled with air). To establish the initial conditions, the PANDA vessels were first isolated and individually preconditioned. When the vessels were stabilized with conditions within a specified tolerance

²⁶ RAI 273

band, the connecting valves between them were opened. The PANDA RPV vessel was brought to its prescribed initial (saturated) state with the heater power close to zero. After the valves were opened, the power was quickly increased to the prescribed initial value for the test. Operator actions during specific tests included valving the IC in or out, delayed injection of DW noncondensable and opening and closing the DW-to-WW bypass leakage path.

5.6 PANTHERS

Thermal-hydraulic performance data for a PCC condenser (Figure 5-7) and an IC module (Figure 5-8) that were prototypical for the SBWR were obtained at the PANTHERS test facility in Piacenza, Italy. The IC module (half unit) tested at PANTHERS is also prototypical for the ESBWR but the PCC unit contained about 25% less tubes than the ESBWR PCC. Extrapolation of the PANTHERS PCC test data to the ESBWR is justified by the fact that the ESBWR PCC design is obtained by simply extending the upper and lower headers to accommodate the additional tubes in the exact geometric pattern of the SBWR unit. Since the PANTHERS tests were conducted with full-scale components, there are no scaling distortions to be addressed other than the issue of PCC extrapolation. There is no expected effect from testing only one IC module except, possibly, minor distortions in pool circulation that would have minimal effect on overall heat transfer

The PANTHERS tests were conducted with prototypical flow, pressure, temperature, and inlet noncondensable fractions. The purpose of the tests was to qualify the PCC and IC condenser designs with respect to thermal-hydraulic performance and structural integrity. Figures 5-9 and 5-10 show schematics of the PANTHERS test facility configured for the PCC and IC tests, respectively. A detailed description of the PANTHERS test objectives is given in the ESBWR TAPD [2-1].

The PANTHERS PCC heat transfer data were collected under steady-state conditions. This procedure was justified because the operation of the PCCS under postulated LOCA conditions can be described as a slow transient. Under certain conditions, PCCS operation may become cyclical but the period of the cycles will be long in comparison to the response time of the PCCS. The characteristic response time of a PCC condenser unit is primarily determined by the transit time of the fluid in the tubes and the time constant of the tube wall, both of which are on the order of a few seconds. Thus, the response of the PCC condenser units to changes in inlet and/or boundary conditions is much faster than the response of the large E/SBWR containment volumes that set those conditions.²⁷

5.7 UCB and MIT Condensation Heat Transfer Tests

The condensation of steam from a mixture of steam and noncondensable gases within a vertical tube under conditions expected in the PCC units was investigated in experimental programs conducted at the University of California-Berkeley (UCB) and the Massachusetts Institute of Technology (MIT). These tests encompassed tube geometries and thermodynamic conditions covering the E/SBWR conditions. Data from these tests were used to develop a model for

²⁷ RAI 274

condensation heat transfer in the presence of noncondensibles that was incorporated in TRACG [5-8].²⁸

²⁸ RAI 298

Table 5-1 The ESBWR Related Tests

Test	Purpose	Nominal ESBWR Scale
GIST	Integral GDCS system test	1:1000
GIRAFFE/SIT	Integral GDCS system test	1:800
GIRAFFE/He	Integral long-term containment heat removal tests with lighter-than-steam noncondensable gas	1:800
PANDA	Integral long-term containment heat removal tests	1:50
PANTHERS IC	Structural and heat transfer tests of the IC	Full-scale prototype (One module)
PANTHERS PCC	Structural and heat transfer tests of the PCC	Full-scale prototype (25% less tubes)
UCB MIT	Condensation in the presence of noncondensibles	Single-tube (near full-scale)

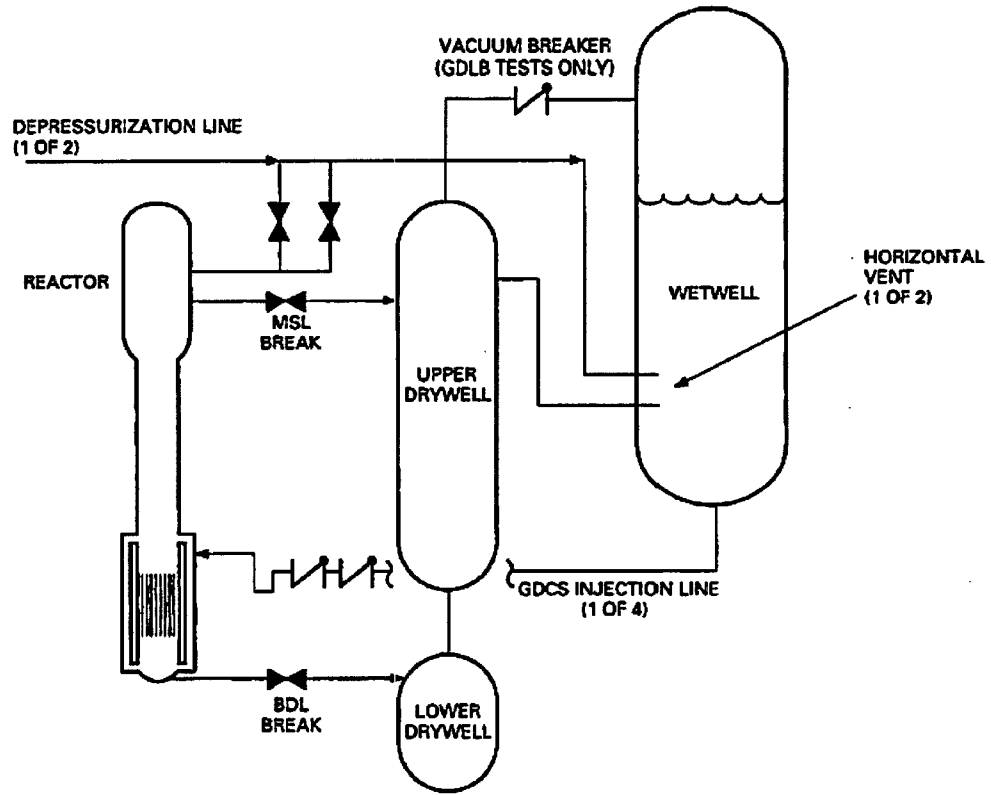


Figure 5.1. Main Components of the GIST Facility

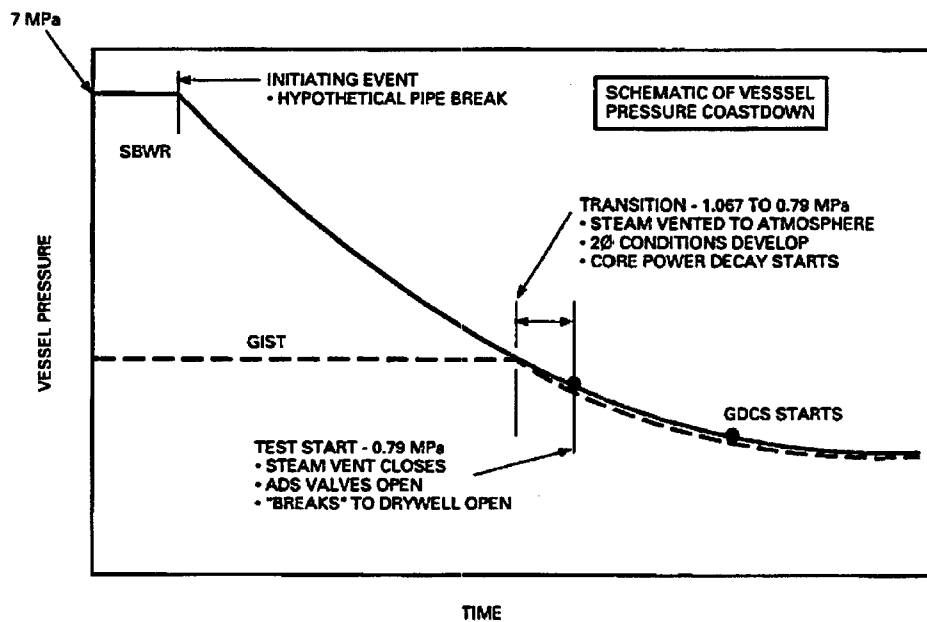
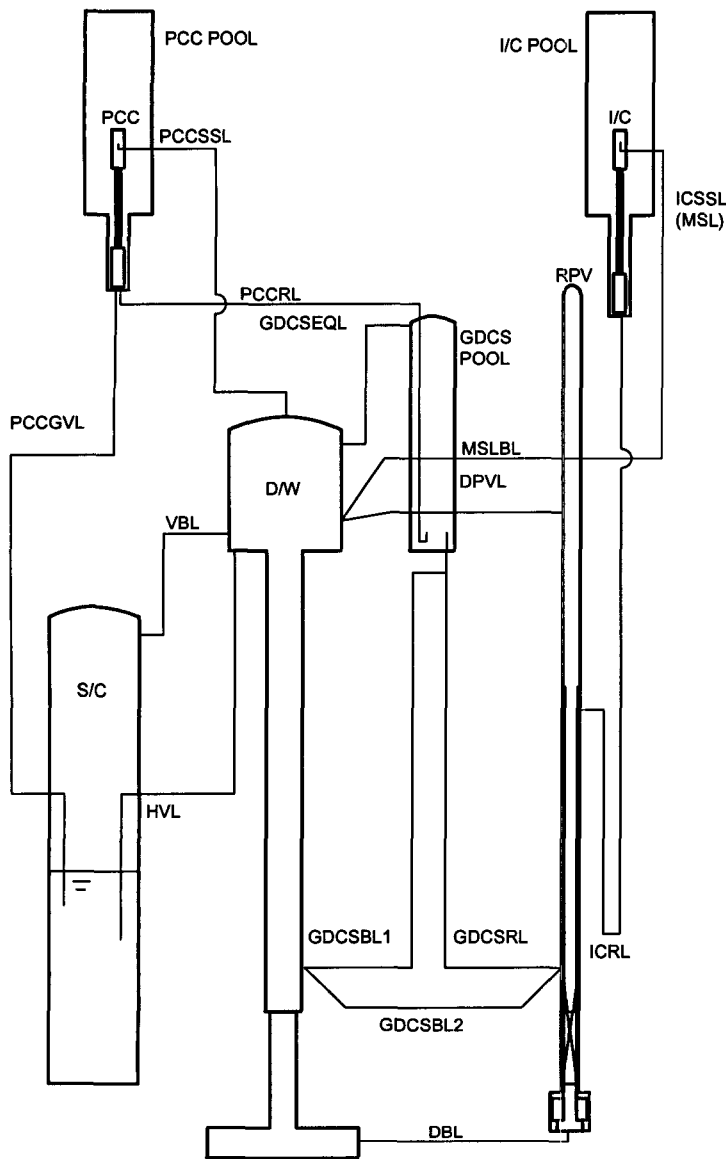


Figure 5.2. Vessel Pressure Coastdown During the SBWR and the GIST Depressurization Transients



- PCCSSL
PCC STEAM SUPPLY LINE
D/W TOP - PCC STEAM BOX
- PCCRL
PCC DRAIN WATER RETURN LINE
PCC WATER BOX - GDCS POOL
WITH U-TUBE
- PCCGVL
PCC GAS VENT LINE
PCC WATER BOX - S/C
- GDCSRL
GDCS DRAIN RETURN LINE
GDCS POOL - RPV
- GDCSEQL
GDCS - D/W PRESSURE
EQUALIZING LINE
GDCS POOL - D/W
- MSBL
MAIN STEAM LINE BREAK LINE
RPV - D/W
- DPVL
DEPRESSURIZATION VALVE LINE
RPV - D/W
- HVL
LOCA (MAIN) VENT LINE
D/W - S/C
- VBL
VACUUM BREAKER LINE
S/C - D/W
- ICSSL
I/C STEAM SUPPLY LINE
RPV - I/C STEAM BOX (MSL)
- ICRL
I/C DRAIN WATER RETURN LINE
I/C WATER BOX - RPV
WITH U-TUBE
- GDCSBL1
GDCSL BREAK LINE
GDCS POOL - D/W
- GDCSBL2
GDCSL BREAK LINE
RPV - D/W
- DBL
BOTTOM DRAIN BREAK LINE
RPV BOTTOM - D/W

Figure 5-3. GIRAFFE Test Facility Schematic (GIRAFFE/SIT Test)

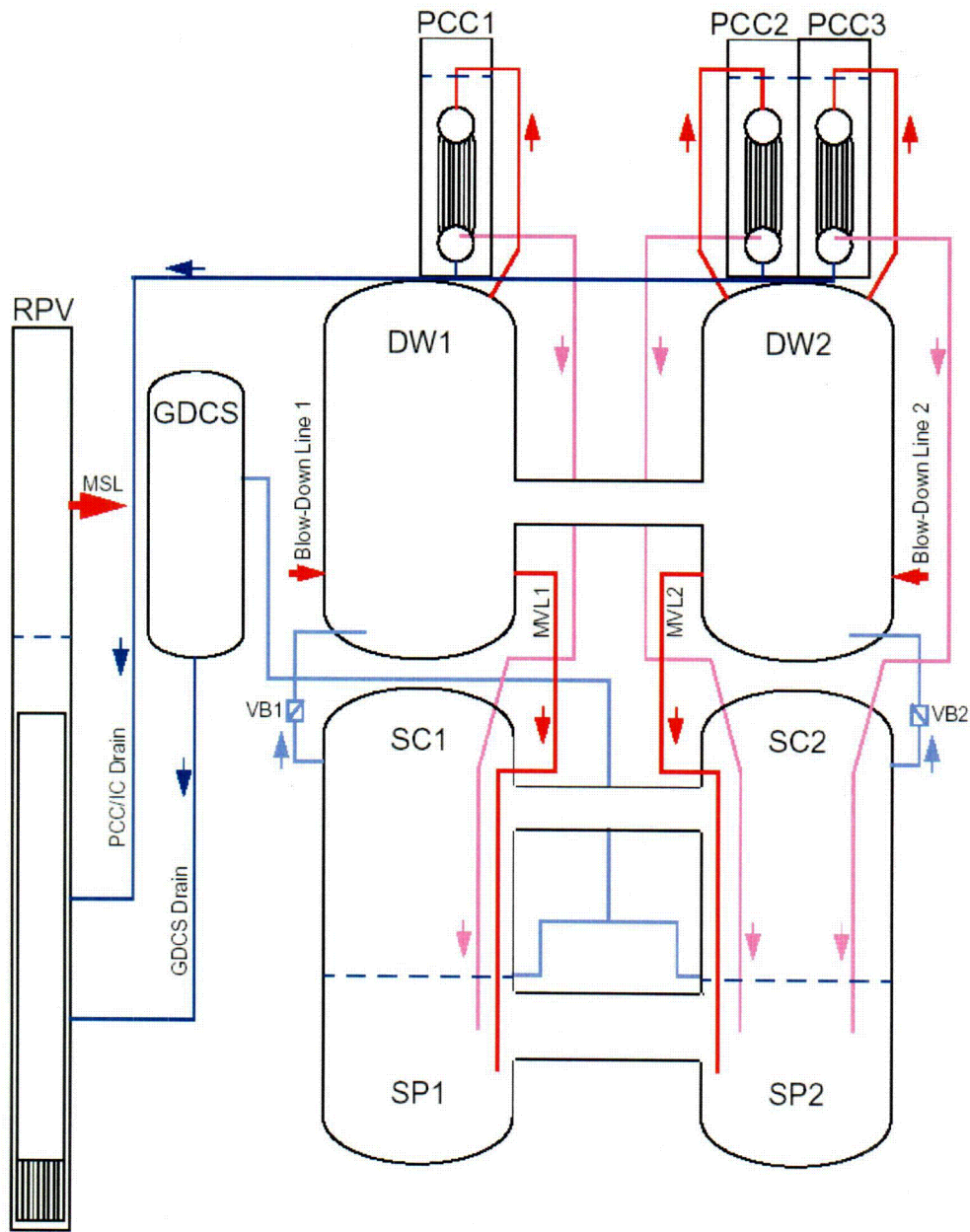


Figure 5-4. PANDA Test Facility Schematic

ESBWR versus PANDA

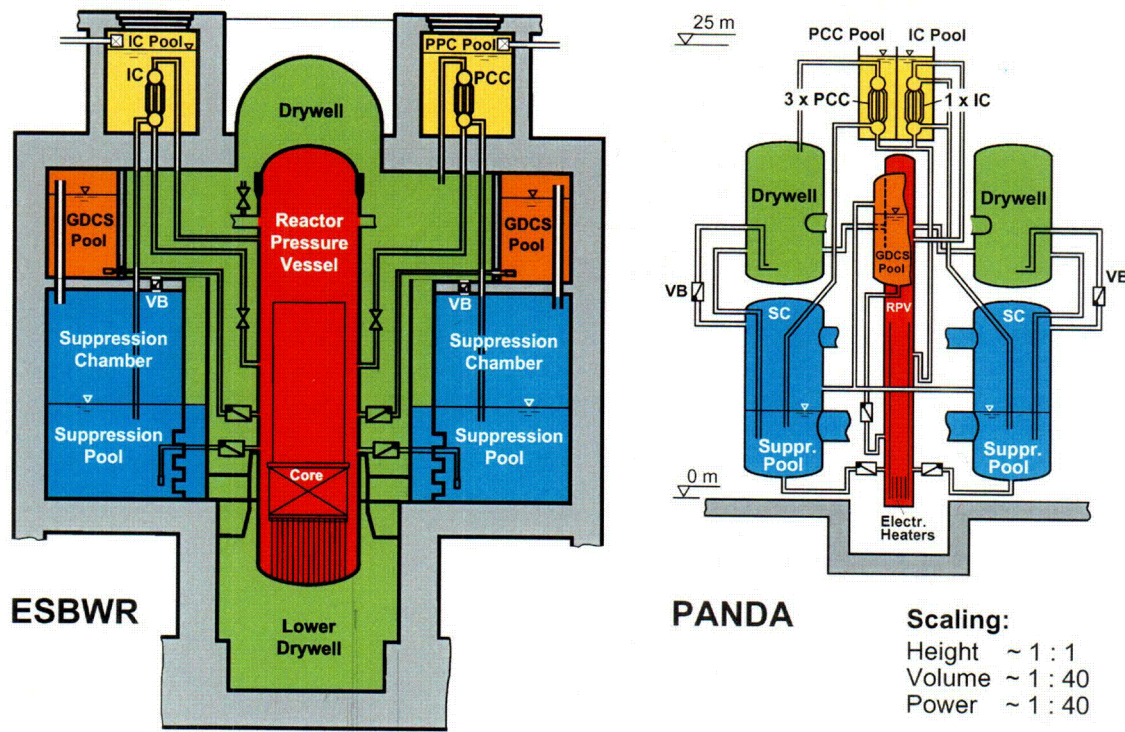


Figure 5-5. Comparison of the PANDA Elevations with the ESBWR

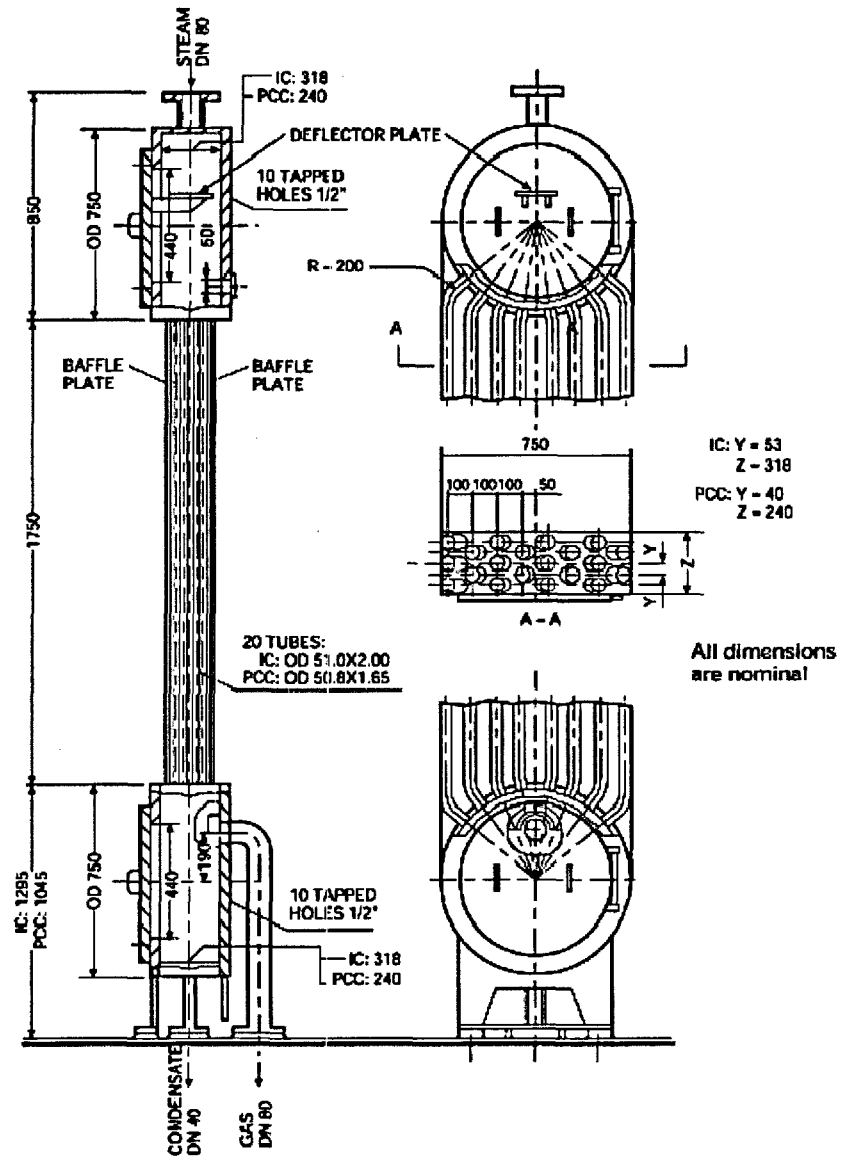


Figure 5-6. The PANDA PCCS and ICS Condenser Units

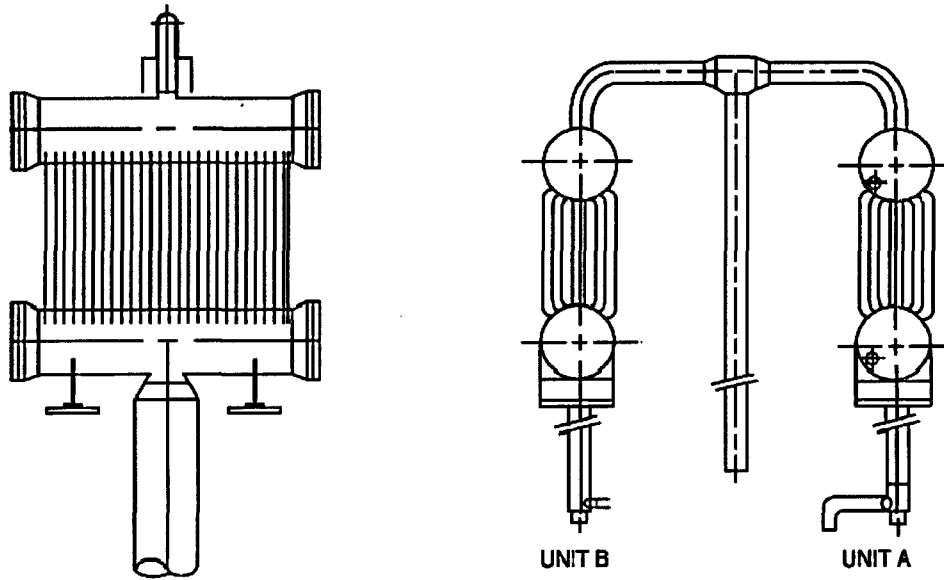


Figure 5-7. Passive Containment Condenser Tested at PANTHERS

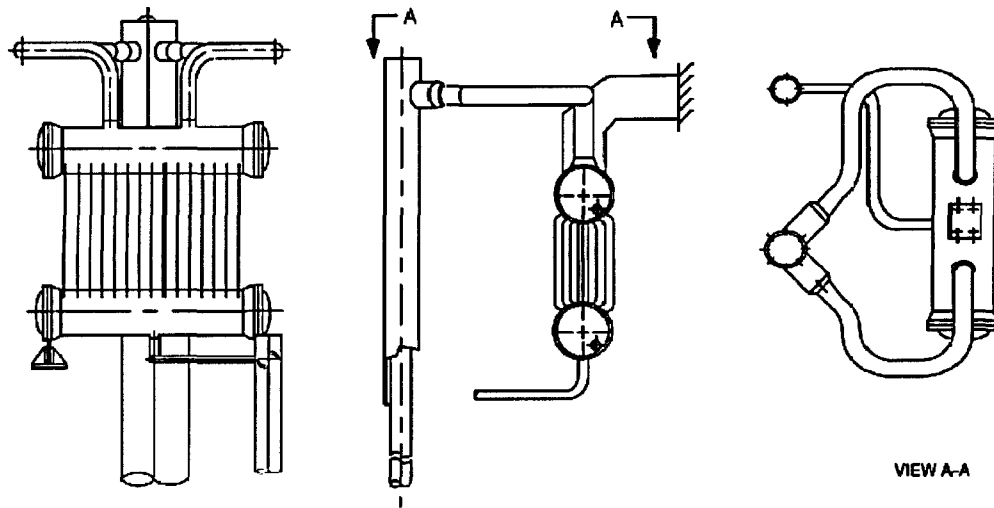


Figure 5-8. Isolation Condenser Module Tested at PANTHERS

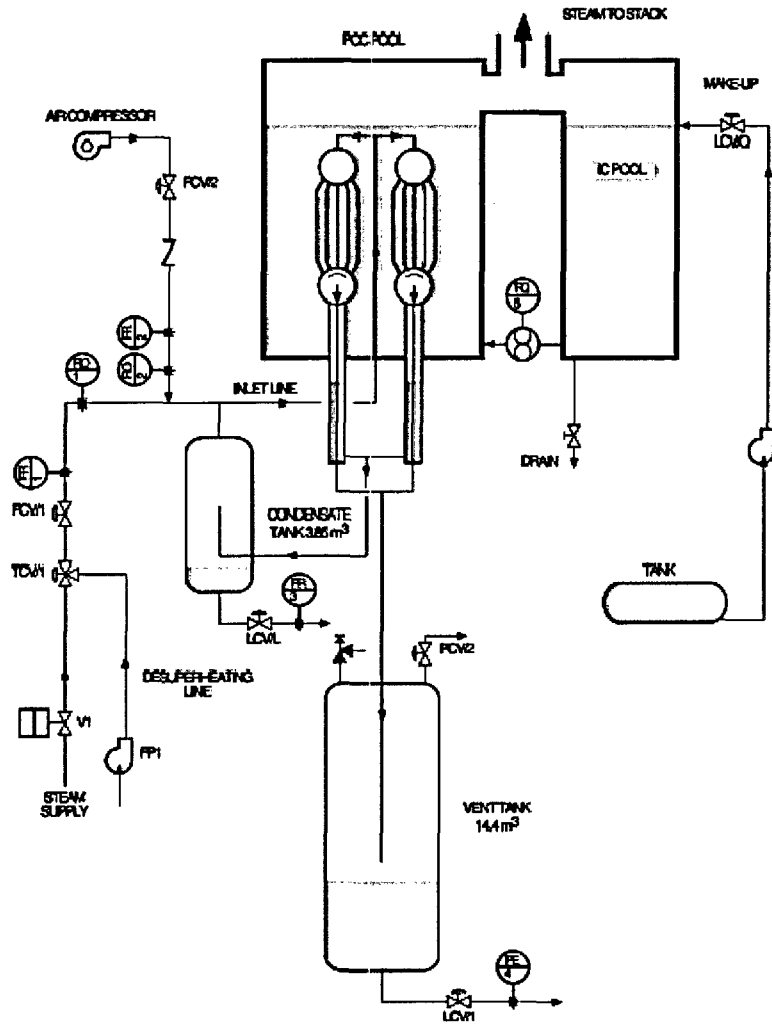


Figure 5-9. Schematic of the PANTHERS PCC Test Facility

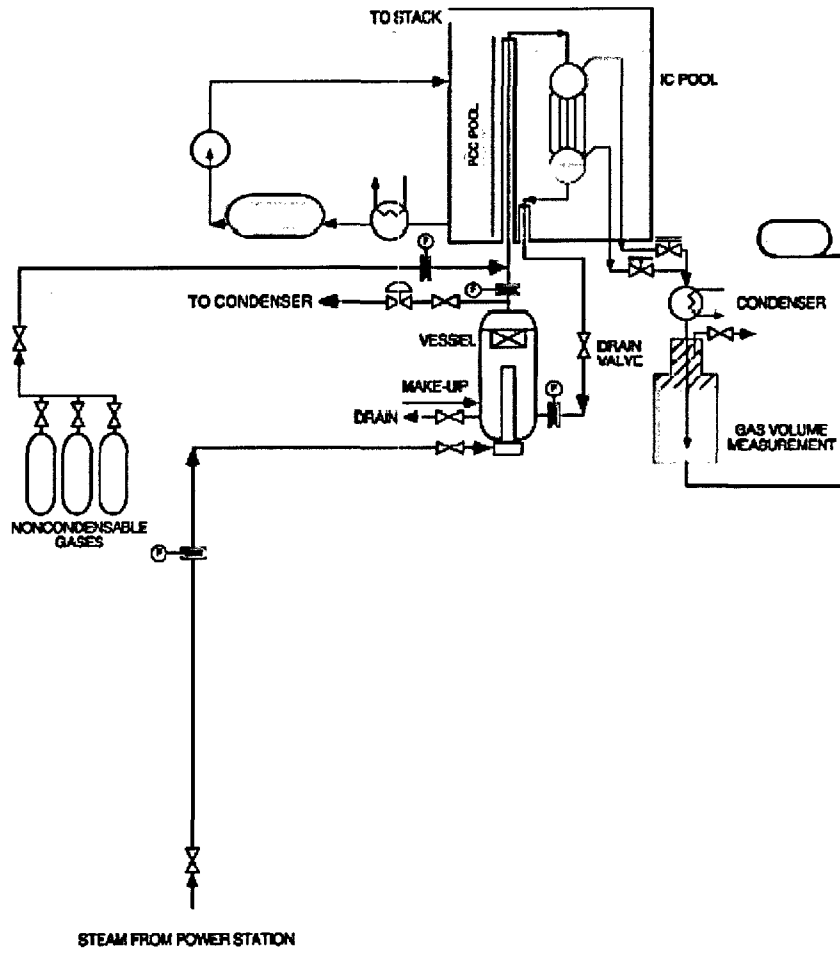


Figure 5-10. Schematics of the PANTHERS IC Test Facility

6.0 SCALING FOR PIRT VALIDATION AND TEST FACILITY EVALUATION

6.1 Scaling for Important Phenomena and Facility Distortions

In Section 4 nondimensionalization of the governing equations resulted in the general scaling criteria used to design the test facilities described in Section 5. However, in practical cases, the models cannot be perfectly scaled. One then needs to evaluate the importance of scaling distortions. This section summarizes a system specific nondimensionalization method that provides the basis for identifying phenomena and processes important to system behavior and identifying distortions that may occur in test facilities.

To properly evaluate the magnitude of scaling distortions, in defining the Π numbers, one should use reference scales making the magnitude of all the *nondimensional* terms of order one. The Π numbers multiplying the various nondimensional terms specify then their relative importance in the governing equation. This information is useful in assessing the effect of scaling distortions, and helps to ensure that (1) all important phenomena are preserved and (2) nonrepresentative effects have not been introduced. In addition, comparing corresponding Π numbers between the test and prototype results in a measure of the distortion for the related phenomenon.

In many systems, several Π groups of the same type appear in the governing equation (for example, several Π groups containing flow rates entering the control volume). It is necessary in these cases to use separate reference values for each term to adequately normalize the different flow rates. The relative magnitude of the resulting Π groups will show which system components should be scaled most carefully. Similarly, the relative magnitude of the Π terms containing the various flow rates will show which component flow rates should be matched most carefully.

Reference values for normalization are selected or carefully calculated using controlled parameters to assure that the nondimensional variables in the model equations will be of order one. For variables that are not differentiated, the reference values are selected as the value at the beginning of the phase. These are denoted by the subscript "o" in the equations below. For differentials, the reference change in the variable is selected using the estimated change resulting from the dominant causative process. These are denoted by the subscript "r" in the equations below. The selection of these reference values is covered in more detail in Section 7.3.

The governing equations summarized in Section 3.3 are normalized using local variables as described above. The resulting nondimensionalized equations are summarized below.

Liquid Mass:

To assess the state of core coverage in the RPV the liquid mass equation is used. This is similar to the void fraction equation used for the general scaling criteria but allows better quantitative assessment of the distortions in test facilities. The development of the equation is shown in Section 4.2.1 and Appendix A of the SBWR Testing Summary Report [3-2]. The right side of the equation contains terms for evaporation due to heat additions, addition of mass by liquid flows, reduction of evaporation due to entering subcooled liquid, and flashing due to depressurization. The nondimensional form of the equation is

$$h_{fg}^+ \frac{dM_{\lambda}^+}{dt^+} = -\sum_k \Pi_{M, \mathcal{E}_k} \mathcal{E}_k^+ + h_{fg}^+ \sum_i \Pi_{M, W, i} W_{\lambda, i}^+ + \sum_i \Pi_{M, sub, i} h_{sub, i}^+ W_{\lambda, i}^+ - \left[\Pi_{M, \mathcal{P}_1} V_{RPV}^+ f_3^+ + \Pi_{M, \mathcal{P}_2} f_4^+ M_{\lambda}^+ \right] \frac{dP^+}{dt^+} \quad (6.1-1)$$

where

$$f_3 = 1 - \rho_g h'_g; \quad f_4 = \frac{\rho_g}{\rho_l} h'_g - h'_f \quad \text{are thermodynamic properties,}$$

$$\begin{aligned} \Pi_{M, \mathcal{E}_k} &= \frac{\mathcal{E}_{k, o}}{h_{fg, o}} \frac{t_r}{\Delta M_{\lambda, r}} \\ \Pi_{M, W, i} &= W_{\lambda, i, o} \frac{t_r}{\Delta M_{\lambda, r}} \\ \Pi_{M, sub, i} &= \frac{\Delta h_{sub, i, o}}{h_{fg, o}} \frac{W_{\lambda, i, o} t_r}{\Delta M_{\lambda, r}} \\ \Pi_{M, \mathcal{P}_1} &= \frac{V_{RPV, o} f_{3, o}}{h_{fg, o}} \frac{\Delta P_r}{\Delta M_{\lambda, r}} \\ \Pi_{M, \mathcal{P}_2} &= \frac{f_{4, o} \Delta P_r}{h_{fg, o}} \frac{M_{\lambda, o}}{\Delta M_{\lambda, r}} \end{aligned} \quad (6.1-2)$$

are PI numbers, and

$$\begin{aligned} \Delta M_{\lambda}^+ &= \frac{M_{\lambda} - M_{\lambda, o}}{\Delta M_{\lambda, r}}; \quad t^+ = \frac{t}{t_r}; \quad \mathcal{E}_k^+ = \frac{\mathcal{E}_k}{\mathcal{E}_{k, o}}; \quad W_{\lambda, i}^+ = \frac{W_{\lambda, i}}{W_{\lambda, i, o}}; \quad h_{sub, i}^+ = \frac{\Delta h_{sub, i}}{\Delta h_{sub, i, o}}; \\ M_{\lambda}^+ &= \frac{M_{\lambda}}{M_{\lambda, o}}; \quad P^+ = \frac{P - P_o}{\Delta P_r}; \quad h_{fg}^+ = \frac{h_{fg}}{h_{fg, o}}; \quad f_3^+ = \frac{f_3}{f_{3, o}}; \quad f_4^+ = \frac{f_4}{f_{4, o}} \end{aligned}$$

are the nondimensional variables. A standard nomenclature for the Π groups is adopted where the first subscript indicates the equation to which the term applies (i.e. mass, pressure), the second one indicates the phenomena represented and the third one indicates the flow path or source.²⁹

²⁹ RAI 280

Temperature (Energy) Equation:

The temperature of the suppression pool is important to the steam partial pressure in the WW gas space. The temperature change is of course dependent on the energy in the pool. The nondimensional form of the full equation is

$$M^+ \frac{de^+}{dt^+} = -\Pi_{e,v} P^+ \frac{dV^+}{dt^+} + \sum_k \Pi_{e,\&k} \&k^+ + \sum_i \Pi_{e,wh,i} W_i^+ h_i^+ + P^+ / \rho^+ \sum_i \Pi_{e,mech,i} W_i^+ \quad (6.1-3)^{30}$$

where:

$$\Pi_{e,v} = \frac{P_o \Delta V_r}{M_o \Delta e_r} ; \Pi_{e,\&k} = \frac{\&k_{k,o} t_r}{M_o \Delta e_r} ; \Pi_{e,wh,i} = \frac{W_{i,o} \Delta h_{i,o} t_r}{M_o \Delta e_r} ; \Pi_{e,mech,i} = \frac{P_o W_{i,o} t_r}{M_o \Delta e_r \rho_o} \quad (6.1-4)$$

³⁰ RAI 281

and

$$e_i^+ = \frac{e - e_o}{\Delta e_r}; \quad P^+ = \frac{P}{P_o}; \quad dV^+ = \frac{dV}{\Delta V_r}; \quad t^+ = \frac{t - t_o}{t_r};$$

$$\mathcal{Q}_k^+ = \frac{\mathcal{Q}_k}{\mathcal{Q}_{i,o}}; \quad W_i^+ = \frac{W_i}{W_{i,o}}; \quad h_i^+ = \frac{h_i - h}{\Delta h_{i,o}};$$

$$\rho^+ = \frac{\rho}{\rho_o}; \quad M^+ = \frac{M}{M_o}$$

are nondimensional variables.

Time Rate of Pressure Change

An additional parameter that is important for the Late Blowdown/GDCS phase is the RPV pressure. It is important because it determines the time at which injection of GDCS flow to the RPV can begin as well as influencing the two-phase level and quantity of liquid changed to vapor due to flashing. The pressure rate equation is developed in the SBWR scaling report [3-1, Eq. 2.5-3].

The right side of the equation contains terms for energy increase due to heat and enthalpy additions, pressurization due to volume changes and fluid addition and changes in constituent fractions. The nondimensional form of the equation is

$$f_2^+ V^+ \frac{dP^+}{dt^+} = \sum_k \Pi_{P,\mathcal{Q}k} Q_k^+ - \Pi_{P,\mathcal{P}} P^{*+} \frac{dV^+}{dt^+} + \sum_i \Pi_{P,W h_i} W_i^+ h_i^+ + \frac{P^{*+}}{\rho^+} \sum_i \Pi_{P,mech_i} W_i^+ - V^+ \sum_j \Pi_{P,y_j} \left(f_{1,j}^+ \frac{dy_j^+}{dt^+} \right) \quad (6.1-5)$$

where

$$P^* = P + \left. \frac{\partial e}{\partial v} \right|_{P,y_j}$$

$$f_{1,j} = \left. \frac{1}{v} \frac{\partial e}{\partial y_j} \right|_{P,v,y}$$

$$f_2 = \left. \frac{1}{v} \frac{\partial e}{\partial P} \right|_{v,y_j}$$

are thermodynamic properties, and

$$\Pi_{P,\mathcal{Q}k} = \frac{\mathcal{Q}_{k,o}}{V_o f_{2,o}} \frac{t_r}{\Delta P_r}$$

$$\Pi_{P,\&} = \frac{P_o^* \Delta V_r}{\Delta P_r V_o f_{2,o}} \quad (6.1-6)$$

$$\Pi_{P,Wh,i} = \frac{W_{i,o} \Delta h_{i,o}}{V_o f_{2,o} \Delta P_r} \frac{t_r}{\Delta P_r}$$

$$\Pi_{P,mech,i} = \frac{W_{i,o} P_o^*}{V_o f_{2,o} \rho_o} \frac{t_r}{\Delta P_r}$$

$$\Pi_{P,y,j} = \frac{f_{1,j,o} \Delta y_{j,r}}{\Delta P_r f_{2,o}}$$

are PI numbers, and

$$P^+ = \frac{P - P_o}{\Delta P_r}; \quad V^+ = \frac{V}{V_o}; \quad dV^+ = \frac{dV}{\Delta V_r}; \quad t^+ = \frac{t - t_o}{t_r};$$

$$\&_k^+ = \frac{\&_k}{\&_{k,o}}; \quad W_i^+ = \frac{W_i}{W_{i,o}}; \quad h_i^+ = \frac{h_i - h}{\Delta h_{i,o}}; \quad y_j^+ = \frac{y_j - y_{j,o}}{\Delta y_{j,r}};$$

$$P^{*+} = \frac{P^*}{P_o^*}; \quad \rho^+ = \frac{\rho}{\rho_o}; \quad f_{1,j}^+ = \frac{f_{1,j}}{f_{1,j,o}}; \quad f_2^+ = \frac{f_2}{f_{2,o}}$$

are nondimensional variables. This equation is used for the RPV for the late blowdown and GDSCS transition phases and in the containment regions for the long-term phase.

Momentum in Lines:

The equation for momentum in lines has not changed from the one used for general scaling criteria in Section 4,

$$\Pi_{in} \frac{dW^+}{dt^+} = \Pi_{pd} \Delta P^+ - \Pi_{loss} \frac{W^{+2}}{\rho^+} + \Pi_h \rho^+ H^+ \quad (6.1-7)$$

Where

$$\Pi_{in} \equiv \frac{W_r \left(\frac{L}{a} \right)_r}{\Delta P_r t_r} \quad (6.1-8)$$

$$\Pi_{pd} \equiv \frac{\Delta P_o}{\Delta P_r} \quad (6.1-9)$$

$$\Pi_{loss} \equiv \frac{W_r^2 \left(\frac{F}{a^2} \right)_r}{2 \Delta P_r \rho_r} \quad (6.1-10)$$

$$\Pi_h \equiv \frac{\rho_r g H_r}{\Delta P_r} \quad (6.1-11)$$

are PI numbers, and

³² RAI 284

³³ RAI 282

$$dW^+ = \frac{W - W_o}{\Delta W_r}; \quad \Delta P^+ = \frac{P_1 - P_2}{\Delta P_o}; \quad t^+ = \frac{t}{t_r}$$

$$W^+ = \frac{W}{W_r}; \quad \rho^+ = \frac{\rho}{\rho_o}; \quad H^+ = \frac{H}{H_o}$$

6.2 Global Momentum Scaling

In the SBWR scaling report [3-1] global momentum scaling was developed and applied. In this process, matrix equations for the entire system are developed and nondimensionalized. In addition, global reference values as well as local ones are used to nondimensionalize the equations. There are two main objectives of this type of scaling:

- identify any additional nondimensional numbers that may result
- identify any interactions between different flow paths that may occur

The results from the SBWR work showed that there are no significant interactions in the SBWR system or the related tests and no new PI numbers resulted.³⁴ In addition, the complexity added by using matrix momentum equations rather than individual equations for each system line made the conclusions that could be drawn regarding momentum scaling less clear.

The ESBWR configuration is similar enough to the SBWR that conclusions resulting from application of this method would be the same. Therefore global momentum scaling is not repeated for the ESBWR in this new work. Instead, the effect on momentum scaling of individual lines that may result from changes to the SBWR design are considered.

6.3 Summary

This section summarized the system specific nondimensionalization of the governing equations for determination of phenomena importance and quantification of distortions in test facilities. The equations are summarized below and the resulting PI numbers are summarized in table 6-1.

These equations are applied to the specific regions of the ESBWR in Section 7 and the test facilities in Section 8.

³⁴ RAI 286, Supp RAI 259 & Supp RAI 286

$$h_{fg}^+ \frac{dM_{\lambda}^+}{dt^+} = -\sum_k \Pi_{M,\&k} \&k^+ + h_{fg}^+ \sum_i \Pi_{M,W,i} W_{\lambda,i}^+ + \sum_i \Pi_{M,sub,i} h_{sub,i}^+ W_{\lambda,i}^+ - [\Pi_{M,\&1} V_{RPV}^+ f_3^+ + \Pi_{M,\&2} f_4^+ M_{\lambda}^+] \frac{dP^+}{dt^+} \quad (6.1-1)$$

(6.1-3)³⁵

$$M^+ \frac{de^+}{dt^+} = -\Pi_{e,\&1} P^+ \frac{dV^+}{dt^+} + \sum_k \Pi_{e,\&k} \&k^+ + \sum_i \Pi_{e,wh,i} W_i^+ h_i^+ + \frac{P^+}{\rho^+} \sum_i \Pi_{e,mech,i} W_i^+$$

$$f_2^+ V^+ \frac{dP^+}{dt^+} = \sum_k \Pi_{P,\&k} Q_k^+ - \Pi_{P,\&1} P^{*+} \frac{dV^+}{dt^+} + \sum_i \Pi_{P,wh,i} W_i^+ h_i^+ + \frac{P^{*+}}{\rho^+} \sum_i \Pi_{P,mech,i} W_i^+ - V^+ \sum_j \Pi_{P,y,j} \left(f_{1,j}^+ \frac{dy_j^+}{dt^+} \right) \quad (6.1-5)$$

$$\Pi_{in} \frac{dW^+}{dt^+} = \Pi_{pd} \Delta P^+ - \Pi_{loss} \frac{W^{+2}}{\rho^+} + \Pi_h \rho^+ H^+ \quad (6.1-7)$$

³⁵ RAI 281

Table 6-1 Summary of PI-groups

PI-group	Equation Where Used	Comment
$\Pi_{M,\&i} = \frac{\&_{i,o} t_r}{h_{fg,o} \Delta M_r}$	Liquid Mass (6.1-1)	Mass loss due to boiling from heat addition
$\Pi_{M,W,i} = W_{\lambda,i,o} \frac{t_r}{\Delta M_{\lambda,r}}$	Liquid Mass (6.1-1)	Mass change due to liquid flow in or out of control volume
$\Pi_{M,sub,i} = \frac{\Delta h_{sub,i,o} W_{\lambda,i,o} t_r}{h_{fg,o} \Delta M_{\lambda,r}}$	Liquid Mass (6.1-1)	Mass change due to subcooling of inlet flow
$\Pi_{M,\&1} = \frac{V_{RPV,o} f_{3,o} \Delta P_r}{h_{fg,o} f_{fg,o} \Delta M_{\lambda,r}}$	Liquid Mass (6.1-1)	Mass change due to flashing as a result of pressure changes (Part 1)
$\Pi_{M,\&2} = \frac{f_{4,o} \Delta P_r M_{\lambda,o}}{h_{fg,o} \Delta M_{\lambda,r}}$	Liquid Mass (6.1-1)	Mass change due to flashing as a result of pressure changes (Part 2)
$\Pi_{e,\&} = \frac{P_o \Delta V_r}{M_o \Delta e_r}$	Temperature (Energy) 6.1-3	Energy change due to changes on volume
$\Pi_{e,\&i} = \frac{\&_{i,o} t_r}{M_o \Delta e_r}$	Temperature (Energy) 6.1-3	Energy change due to heat additions
$\Pi_{e,wh,i} = \frac{W_{i,o} \Delta h_{i,o} t_r}{M_o \Delta e_r}$	Temperature (Energy) 6.1-3	Energy change due to enthalpy additions
$\Pi_{e,mech,i} = \frac{P_o W_{i,o} t_r}{M_o \Delta e_r \rho_o}$	Temperature (Energy) 6.1-3	Energy changes due to mechanical work from incoming fluid
$\Pi_{P,\&i} = \frac{\&_{i,o} t_r}{V_o f_{2,o} \Delta P_r}$	Pressure Rate (6.1-5)	Pressure change due to sensible heat additions
$\Pi_{P,\&} = \frac{P_o^* \Delta V_r}{\Delta P_r V_o f_{2,o}}$	Pressure Rate (6.1-5)	Pressure change due to compression by volume changes
$\Pi_{P,wh,i} = \frac{W_{i,o} \Delta h_{i,o} t_r}{V_o f_{2,o} \Delta P_r}$	Pressure Rate (6.1-5)	Pressure change due to enthalpy additions
$\Pi_{P,mech,i} = \frac{W_{i,o} P_o^* t_r}{V_o f_{2,o} \rho_o \Delta P_r}$	Pressure Rate (6.1-5)	Pressure change due to mechanical work from incoming fluid
$\Pi_{P,y,j} = \frac{f_{1,j,o} \Delta y_{j,r}}{\Delta P_r f_{2,o}}$	Pressure Rate (6.1-5)	Pressure change due to changes in constituent mass fractions
$\Pi_{in} \equiv \frac{W_r \left(\frac{L}{a} \right)_r}{\Delta P_r t_r}$	Momentum (6.1-7)	Ratio of pressure drop due to acceleration to reference pressure drop

PI-group	Equation Where Used	Comment
$\Pi_{pd} \equiv \frac{\Delta P_o}{\Delta P_r}$	Momentum (6.1-7)	Ratio of pressure difference between end points to reference pressure drop
$\Pi_{loss} \equiv \frac{W_r^2 \left(\frac{F}{a^2} \right)_r}{2\Delta P_r \rho_r}$	Momentum (6.1-7)	Ratio of pressure drop due to friction and form basis to reference pressure drop
$\Pi_h \equiv \frac{\rho_r g H_r}{\Delta P_r}$	Momentum (6.1-7)	Ratio of submergence or hydrostatic pressure difference to reference pressure drop

7.0 ESBWR RESULTS – PIRT VALIDATION

In this section the nondimensional form of the governing equations summarized in Section 6 are applied to the ESBWR.³⁶ Sections 7.1 and 7.2 discuss the transient phases of a LOCA in the ESBWR and for what periods, ESBWR volumes, and parameters the scaling will be applied. Section 7.3 summarizes the method of selecting reference that assures that the scaling results obtained are valid. In Sections 7.4 through 7.7 the results are presented and summarized for the equations to the ESBWR. The details of the reference values used and detailed results can be found in Appendix A.

7.1 Transient Phases

Figure 1-1 shows the different periods or phases of a LOCA transient in the ESBWR. Key variables are represented schematically in the figure (RPV, DW and WW pressures; decay heat and PCC heat removal; GDCS flow and RPV mass). The figure shows how the magnitudes of the different parameters vary from phase to phase. Four transient phases were considered for scaling: (1) Late Blowdown, (2) Transition to GDCS Flow, (3) Full GDCS (or Reflood), and (4) Long Term PCCS. The breaks between phases were selected based on when a significant change in the magnitude of one or more of the key variables occurred. Within each phase, the important variables maintain a similar magnitude and/or the same phenomena remain important. Breaking the transient into phases is necessary to assure that the nondimensional variables remain of order one over the range of application, which is a necessary condition for validity of the top-down scaling methodology as has been discussed in [7-1]. Scaling provides a snapshot of the system behavior at a single point in time. By breaking the transient into phases where the magnitudes of variables do not change significantly the scaling done at a single point in time is representative of the entire phase. Therefore scaling in some time dependent way is neither needed nor desirable.

7.2 Important System Parameters³⁷

³⁶ RAI 285

³⁷ RAI 294

Table 7-1 Application of Scaling Equations to ESBWR Phases and Regions³⁸

7.3 Reference Parameters

³⁸ RAI 294

7.3.1 Transient Phase Boundaries

|

|

³⁹ RAI 287
⁴⁰ RAI 288

|

|

| ⁴¹ RAI 289

7.3.2 Reference Times

7.3.3 Pressure

7.3.4 Flow rates

7.4 Format of Results

7.5 Top-Down Results

7.5.1 RPV Behavior

⁴² RAI 290

7.5.2 Containment behavior

7.5.2.1 Drywell Pressure Rate

|

|

7.5.2.2 Wetwell Pressure Rate

7.5.2.3 Passive Containment Cooling System (PCCS)

7.5.3 Summary of Top-down Results

7.6 Bottom-up Scaling

|

|

|

|

⁴³ RAI 259.1

⁴⁴ RAI 283

⁴⁵ RAI 291

Figure 7-1. ESBWR - RPV Late Blowdown: Time Rate of Liquid Mass Change (Mdot)

Figure 7-2. ESBWR - RPV GDCS Transition: Time Rate of Liquid Mass Change (Mdot)

Figure 7-3. ESBWR – RPV Full GDCS (Reflood): Time Rate of Liquid Mass Change (Mdot)

Figure 7-4. ESBWR – RPV Late Blowdown: Time Rate of Pressure Change (Pdot)

Figure 7-5. ESBWR – RPV GDCS Transition: Time Rate of Pressure Change (Pdot)

Figure 7-6. ESBWR – Drywell Long Term/PCCS: Time Rate of Pressure Change (Pdot)

Figure 7-7. ESBWR – Wetwell Long Term/PCCS: Time Rate of Pressure Change (Pdot)

8.0 TEST FACILITY SCALING

Table 8-1 Numerical Scaling Evaluations

8.1 Criteria for Well Scaled Facility

8.2 Reference Parameters

8.3 Short-term RPV Behavior

⁴⁶ RAI 295

⁴⁷ RAI 292 & Supp. RAI 292

8.4 Long-term

⁴⁸ RAI 293

8.5 PCC Scaling

8.6 Summary for Test Facility Comparison

⁴⁹ RAI 14

Figure 8-1. RPV Late Blowdown: Time Rate of Liquid Mass Change (Mdot) - Summary

Figure 8-2. RPV GDCS Transition: Time Rate of Liquid Mass Change (Mdot) - Summary

Figure 8-3. RPV Full GDCS (Reflood): Time Rate of Liquid Mass Change (Mdot) - Summary

Figure 8-4. RPV Late Blowdown: Time Rate of Pressure Change (Pdot) - Summary

Figure 8-5. RPV GDCS Transition: Time Rate of Pressure Change (Pdot) – Summary

Figure 8-6. Drywell Long Term/PCCS: Time Rate of Pressure Change (Pdot) – Summary

Figure 8-7. Wetwell Long Term/PCCS: Time Rate of Pressure Change (Pdot) - Summary

9.0 EFFECT OF SCALE

|

|

| ⁵⁰RAI 13

Figure 9-1 Nondimensional RPV Pressure Comparison for SBWR, GIRAFFE/SIT and GIST

Figure 9-2 Nondimensional RPV Liquid Mass Comparison for SBWR, GIRAFFE/SIT and GIST

Figure 9-3 Comparison of WW Pressure Increases with Noncondensable Partial Pressures for Giraffe/He, PANDA-M and PANDA-P tests

Figure 9-4 Comparison of PCC and IC Behavior for Pure Steam at Different Scales

Figure 9-5 Comparison of PCC Behavior for Steam-Noncondensable Mixtures at Different Scales

10.0 SUMMARY AND CONCLUSIONS

The **objective** of this scaling report is to show that the test facilities properly “scale” the important phenomena and processes identified in the ESBWR PIRT and/or provide assurance that the experimental observations from the test programs are sufficiently representative of ESBWR behavior for use in qualifying TRACG for ESBWR licensing calculations. This objective is met through a series of steps described below.

Section 2 provides an overview of the methodology used. The scaling methodology follows the hierarchical two-tiered scaling methodology composed of top-down scaling, which identifies processes important to the system behavior and a bottom-up, or phenomena level, scaling that looks at the characteristics of the processes identified as important from the top-down scaling

Section 3 describes the equations that govern the behavior of parameters important to the behavior and safety of the ESBWR, namely: RPV liquid mass, pressure and void fraction; containment pressure; and suppression pool energy. These equations are normalized in subsequent sections to provide scaling laws and evaluate the ESBWR and test facilities.

In **Section 4** the system governing equations are normalized using general reference parameters in order to arrive at a set of **general scaling criteria** that can be used for test facility design. These are the criteria that were used for the design of the test facilities included in this report. **Brief descriptions of the test facilities** are provided in **Section 5** as well as references to where the details of the test facilities can be found. In general the design of the experimental facilities and the conduct of the various tests were guided by consideration of the proper modeling and simulation of the key phenomena governing the performance of the passive safety systems. The implications of the scaling adjustments for the ESBWR are minimized by the fact that all of the tests were performed at prototypical temperature and pressure and with prototypical or near-prototypical elevations and elevation differences. These are the key variables and parameters governing the performance of the passive safety systems.

It should be noted that the general scaling criteria are very useful for facility design but do not provide a measure of what phenomena are important to the system behavior, nor are they useful in identifying distortions in the test facilities once they are completed. Instead this is accomplished with a more detailed nondimensionalization of the governing equations as described in **Section 6**. The nondimensionalization developed in Section 6 provides detailed scaling equations that can be used to identify which phenomena are important to the system behavior and therefore should be well scaled in the test facilities. Additionally these equations can be used to assess if this goal had been achieved in the tests.

In **Section 7** the detailed scaling equations from Section 6 are applied to the ESBWR to identify the processes important to the system behavior. The parameters important to safety are identified as: the RPV liquid mass that ensures that the core remains covered; the RPV pressure which is important in determining the timing of the GDCS injection; and the containment pressure which is important to assure that the containment is not breached during an accident. The LOCA transient is broken down into four temporal phases – late blowdown, GDCS transition, reflood, and long-term decay heat removal – within which the dominant phenomena remain unchanged and the phenomena magnitudes are relatively constant.

The **results for the ESBWR** indicate that a small number of processes are important to the behavior of the system parameters of interest (liquid mass and pressure). For the RPV liquid mass the important processes are flashing due to depressurization, boiling due to energy input from stored energy and decay heat, and GDCS flow (Figures 7-1 through 7-3). Although other parameters influence the behavior of the liquid mass during the short GDCS transition phase, the mass change during this phase is very small and therefore not very significant to the overall mass loss in the vessel. For the RPV pressure the dominant phenomena is energy flow through the ADS system (Figures 7-4 and 7-5).

The wetwell pressure controls the containment pressure and the drywell is found to be unimportant to the containment response during the transient period considered (late blowdown onward). The drywell is found to act in a manner similar to a large pipe that transfers steam from the RPV to the main vents and PCCs (Figure 7-6). The time constant for the DW pressure is very short compared to the wetwell and the pressure in the DW therefore rapidly adjusts to the boundary condition presented by the WW pressure. The primary contribution of the DW is that its volume determines the quantity of noncondensable gas that must be accommodated by the WW in the long term. The important process for the containment pressure is the movement of noncondensable gas from the DW to the WW (Figure 7-7).

In **Section 8**, the same scaling method is applied to the test facilities to evaluate if the phenomena identified as important to the ESBWR are scaled properly in the test facilities. Figures 8-1 through 8-7 show that all of the important phenomena magnitudes are well scaled in the test facilities.

Proper bottom-up scaling is a common problem with reduced scale facilities, where aspect ratio, surface to volume ratio and other geometric considerations make it difficult to simulate local effects. A review of the processes important to the system behavior concludes that they are either well scaled from the bottom-up perspective (ADS flow, PCC heat removal, SP mixing) or can be addressed through parametric studies and a bounding approach with TRACG (stratification in gas space, SP mixing). Much of the bottom-up results are borrowed from the SBWR scaling report rather than repeating them in this report.⁵¹

Although it does not constitute scaling analyses, **absence of significant distortions is confirmed** by comparing key parameters from tests done at a wide variety of scales in **Section 9**. The comparisons shown in Figures 9-1 through 9-5 show a similar behavior at all scales indicating that the important processes were well represented in the tests and that no significant scale distortions occurred.

The conclusions drawn from this report and results of the tests are:

- There are only a small number of phenomena important to ESBWR system behavior
- Important phenomena are well scaled in the tests

⁵¹ RAI 15

- No unexpected phenomena were observed in the tests*
- Distortions in localized phenomena (bottom-up) due to reduced scale facilities were not significant
- Comparison of test results at different scales confirm these results

Overall the test facilities are demonstrated to adequately simulate the phenomena important to the ESBWR. Although there are distortions in the facilities, they are found to be in areas that do not affect significant parameters for the system behavior. As such, the test data obtained from these facilities are suitable for qualification of TRACG.

* some non prototypic heat leakage from the man vent pipe to the WW gas space for portions of the PANDA P tests resulted in non representative phenomena for short periods. Once observed, they were eliminated by closing the main vent valve (see the ESBWR Test Summary [10-1] for details)

11.0 REFERENCES

- [1-1] ESBWR Design Description, NEDC-33084P, Rev 1, August 2003 .
- [1-2] ESBWR Test and Analysis Program Description, NEDC-33079P, August 2002.
- [2-1] Zuber, N., *Hierarchical, Two-Tiered Scaling Analysis Appendix D to An Integrated Structure and Scaling Methodology for Severe Accident Technical Issue Resolution*, Nuclear Regulatory Commission Report NUREG/CR-5809, EGG-2659, November 1991.
- [3-1] R. E. Gamble, et al., *Scaling of the SBWR Related Tests*, NEDC-32288P, Revision 1, October 1995.
- [3-2] P.F. Billig, et al., *SBWR Testing Summary Report*, NEDC-32606P Revision 0, August 2002.
- [4-1] Boucher, T.J., diMarzo, M., and Shotkin, L.M., *Scaling Issues for a Thermal-Hydraulic Integral Test Facility*, 19th Water Reactor Safety Information Meeting, Washington, DC, October 30, 1991.
- [4-2] Ishii, M. and Kataoka, I., *Similarity Analysis and Scaling Criteria for LWR's Under Single-Phase and Two-Phase Natural Circulation*, NUREG/CR-3267, ANL-83-32, 1983.
- [4-3] Kiang, R.L., *Scaling Criteria for Nuclear Reactor Thermal Hydraulics*, Nucl. Sci. and Eng., 89, 207-216, 1985.
- [4-4] Kocamustafaogullari G. and Ishii, M., *Scaling Criteria for Two-Phase Flow Loops and their Application to Conceptual 2x4 Simulation Loop Design*, Nucl. Tech., 65, 146-160, 1984.
- [4-5] G. Yadigaroglu *Derviation of General Scaling Criteria for BWR Containment Tests* 4th International Conference on Nuclear Engineering, New Orleans, LA, March 13-14, 1996.
- [5-1] *TRACG Qualification for SBWR*, NEDC-32725P, Rev. 1, August 2002.
- [5-2] *TRACG Qualification for ESBWR*, NEDC-33080P, August 2002.
- [5-3] J. G. M. Andersen et al., *TRACG Qualification*, Licensing Topical Report, NEDE-32177P, Rev. 2, January 2000.
- [5-4] *Mark III LOCA-Related Hydrodynamic Load Definition*, Nuclear Regulatory Commission Report NUREG 0978, August 1984.
- [5-5] P. F. Billig, *Simplified Boiling Water Reactor (SBWR) Program Gravity-Driven Cooling System (GDSCS) Integrated Systems Test – Final Report*, GE Nuclear Energy Report GEFR-00850, October 1989.

- [5-6] P. F. Peterson, V. E. Schrock., and R. Greif., *Scaling for Integral Simulation of Mixing in Large, Stratified Volumes*, NURETH 6, Proc. Sixth Int. Topical Meeting on Nuclear Reactor Thermal Hydraulics, 5-8 Oct. 1993, Grenoble, France, Vol. 1, pp. 202-211.
- [5-7] S. Lomperski, *PANDA Facility Characterization Vessel Heat Loss Measurements*, ALPHA-519-0, November 1997.
- [5-8] K. M. Vierow and V. E. Schrock, *Condensation in a Natural Circulation Loop with Noncondensable Gases-Part I – Heat Transfer*, Proc. Of the Int. Conf. On Multiphase Flows, V. 1, pp. 183-190, Tsukuba, Japan, September 1991.
- [7-1] W. Wulff, U.S. Rohatgi *System Scaling for the Westinghouse AP600 Pressurized Water Reactor and Related Test Facilities*, NUREG-SS-11, BNL-NUREG-52550, September 1997.
- [8-1] *GIRAFFE SBWR System Interaction Test Report*, NEDC-32504P, June 1996.
- [8-2] B. S. Shiralkar, et.al., *TRACG Application for ESBWR*, NEDC-33083P, November 2002
- [10-1] J. R. Fitch, et al, *ESBWR Test Report*, NEDC-33091P, August 2002.

Appendix A – Detailed Results⁰

ENCLOSURE 3

MFN 06-013

Affidavit

General Electric Company

AFFIDAVIT

I, George B. Stramback, state as follows:

- (1) I am Manager, Regulatory Services, General Electric Company ("GE") and have been delegated the function of reviewing the information described in paragraph (2) which is sought to be withheld, and have been authorized to apply for its withholding.
- (2) The information sought to be withheld is contained in the GE proprietary report, NEDC-33082P, Revision 1, *ESBWR Scaling Report*, January 2006. GE proprietary information is identified by sidebars in the right margin adjacent to the proprietary material. Each page of the report contains the designation, "GE Proprietary Information ^{3}" The superscript notation ^{3} refers to Paragraph (3) of this affidavit, which provides the basis for the proprietary determination.
- (3) In making this application for withholding of proprietary information of which it is the owner, GE relies upon the exemption from disclosure set forth in the Freedom of Information Act ("FOIA"), 5 USC Sec. 552(b)(4), and the Trade Secrets Act, 18 USC Sec. 1905, and NRC regulations 10 CFR 9.17(a)(4), and 2.790(a)(4) for "trade secrets" (Exemption 4). The material for which exemption from disclosure is here sought also qualify under the narrower definition of "trade secret", within the meanings assigned to those terms for purposes of FOIA Exemption 4 in, respectively, Critical Mass Energy Project v. Nuclear Regulatory Commission, 975F2d871 (DC Cir. 1992), and Public Citizen Health Research Group v. FDA, 704F2d1280 (DC Cir. 1983).
- (4) Some examples of categories of information which fit into the definition of proprietary information are:
 - a. Information that discloses a process, method, or apparatus, including supporting data and analyses, where prevention of its use by General Electric's competitors without license from General Electric constitutes a competitive economic advantage over other companies;
 - b. Information which, if used by a competitor, would reduce his expenditure of resources or improve his competitive position in the design, manufacture, shipment, installation, assurance of quality, or licensing of a similar product;
 - c. Information which reveals aspects of past, present, or future General Electric customer-funded development plans and programs, resulting in potential products to General Electric;

- d. Information which discloses patentable subject matter for which it may be desirable to obtain patent protection.

The information sought to be withheld is considered to be proprietary for the reasons set forth in paragraphs (4)a., and (4)b, above.

- (5) To address 10 CFR 2.390 (b) (4), the information sought to be withheld is being submitted to NRC in confidence. The information is of a sort customarily held in confidence by GE, and is in fact so held. The information sought to be withheld has, to the best of my knowledge and belief, consistently been held in confidence by GE, no public disclosure has been made, and it is not available in public sources. All disclosures to third parties including any required transmittals to NRC, have been made, or must be made, pursuant to regulatory provisions or proprietary agreements which provide for maintenance of the information in confidence. Its initial designation as proprietary information, and the subsequent steps taken to prevent its unauthorized disclosure, are as set forth in paragraphs (6) and (7) following.
- (6) Initial approval of proprietary treatment of a document is made by the manager of the originating component, the person most likely to be acquainted with the value and sensitivity of the information in relation to industry knowledge. Access to such documents within GE is limited on a "need to know" basis.
- (7) The procedure for approval of external release of such a document typically requires review by the staff manager, project manager, principal scientist or other equivalent authority, by the manager of the cognizant marketing function (or his delegate), and by the Legal Operation, for technical content, competitive effect, and determination of the accuracy of the proprietary designation. Disclosures outside GE are limited to regulatory bodies, customers, and potential customers, and their agents, suppliers, and licensees, and others with a legitimate need for the information, and then only in accordance with appropriate regulatory provisions or proprietary agreements.
- (8) The information identified in paragraph (2), above, is classified as proprietary because it contains detailed test results and interpretations of testing performed in different facilities and their applicability to TRACG modeling of passive safety systems in BWR designs. The reporting, evaluation, and interpretations of test results was achieved at a significant cost, on the order of several million dollars, to GE.

The development of the testing and evaluation process along with the interpretation and application of the analytical results is derived from the extensive experience database that constitutes a major GE asset.

- (9) Public disclosure of the information sought to be withheld is likely to cause substantial harm to GE's competitive position and foreclose or reduce the availability of profit-making opportunities. The information is part of GE's

comprehensive BWR safety and technology base, and its commercial value extends beyond the original development cost. The value of the technology base goes beyond the extensive physical database and analytical methodology and includes development of the expertise to determine and apply the appropriate evaluation process. In addition, the technology base includes the value derived from providing analyses done with NRC-approved methods.

The research, development, engineering, analytical and NRC review costs comprise a substantial investment of time and money by GE.

The precise value of the expertise to devise an evaluation process and apply the correct analytical methodology is difficult to quantify, but it clearly is substantial.

GE's competitive advantage will be lost if its competitors are able to use the results of the GE experience to normalize or verify their own process or if they are able to claim an equivalent understanding by demonstrating that they can arrive at the same or similar conclusions.

The value of this information to GE would be lost if the information were disclosed to the public. Making such information available to competitors without their having been required to undertake a similar expenditure of resources would unfairly provide competitors with a windfall, and deprive GE of the opportunity to exercise its competitive advantage to seek an adequate return on its large investment in developing these very valuable analytical tools.

I declare under penalty of perjury that the foregoing affidavit and the matters stated therein are true and correct to the best of my knowledge, information, and belief.

Executed on this 14th day of January 2006


George B. Stramback
General Electric Company